

AD-A141 249

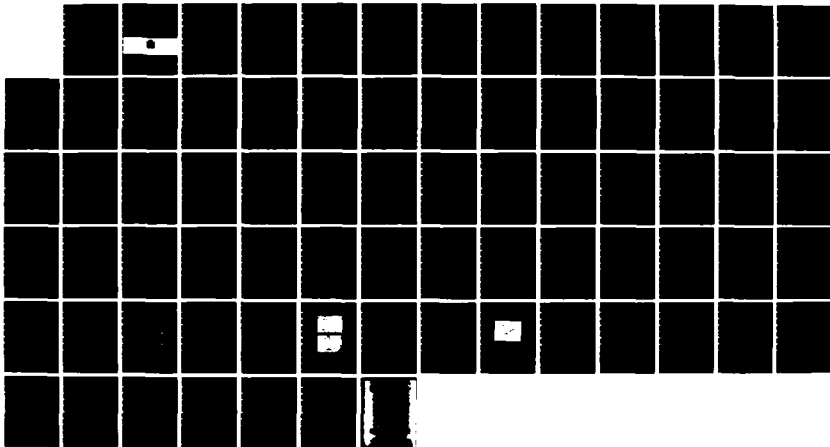
THE ROLE OF TRAPS IN THE MICROSTRUCTURAL CONTROL OF
HYDROGEN EMBRITTLEMEN. (U) CARNEGIE MELLON UNIV
PITTSBURGH PA DEPT OF METALLURGICAL ENGI...
I M BERNSTEIN ET AL. APR 84 TR-17

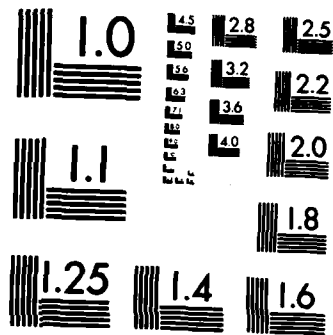
1/1

UNCLASSIFIED

F/G 11/6

NL

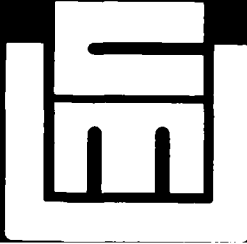




MICROCOPY RESOLUTION TEST CHART
NATIONAL BUREAU OF STANDARDS-1963-A

AD-A141 249

12



Technical Report No. 17

to

Office of Naval Research under
Contract N00014-75-C-0265, NR 036-099 (C-MU)

The Role of Traps in the Microstructural
Control of Hydrogen Embrittlement of Steels

I.M. Bernstein and G.M. Pressouyre*
Dept. of Metallurgical Engineering and Materials Science
Carnegie-Mellon University
Pittsburgh, PA 15213
*Creusot-Loire Research Center
71208 Le Creusot, France



A-1

April 1984

Distribution of this document is unlimited
This work was sponsored by the Metallurgy Branch of the
Office of Naval Research

I. INTRODUCTION:

Since the discovery more than 100 years ago that hydrogen can promote premature failure in steels (1), the pervasiveness of the phenomenon in both ferrous and non-ferrous alloys has prompted innumerable studies to both understand and control "hydrogen embrittlement." It is not the purpose of this article to review in detail the many examples and the many attempts to model the effect, as there are quite a number of recent review articles and conference proceedings devoted to such topics (2)-(10); further, a number of the chapters in this book directly address many of these important points. Instead we will focus our attention on what can be broadly classified as the physical metallurgy of hydrogen effects in ferrous alloys; viz the many different ways by which hydrogen can interact with heterogeneities in the microstructure and the effect of such interactions on the alloy's subsequent ductility or toughness. Such a focus recognizes that it is precisely these local interactions that create the necessary sub steps for failure - crack or void initiation, subsequent growth of the flaw to some critical dimension and finally unstable fast fracture or the link up of subcritical flaws. While in this approach we will address such issues as the need for a localized critical hydrogen concentration, we will not consider how such an accumulation actually triggers premature embrittlement. In other words, we will exclude such mechanistic issues as hydrogen's effects on cohesive strength, triggering of localized plasticity, etc., not because these are not important, but because we believe that currently greater progress can be made by identifying microstructural parameters that can be manipulated to improve performance.

Almost all models share in common the belief that it is hydrogen in its dissociated, dissolved state that is responsible for embrittlement, quite independent of the initial source of the hydrogen, so long as kinetic barriers do not exist. The sequential steps of hydrogen introduction, transport, accumulation and influence on fracture can be visualized in the summary road map of Figure 1, due to Thompson and Bernstein (4), which details the various sub-steps from entry to trapping (or local accumulation)

to premature failure:

Hydrogen may be derived from hydrogen gas molecules which adsorb onto the metal surface and dissociate; by recombination of hydrated protons, H_3O^+ with electrons at the metal surface; or by reaction between hydrogen-containing molecules such as alcohols and the metal (or oxide) surface to release hydrogen. While all of these sources give rise to hydrogen in solution, and while in clearly-defined cases hydrogen gas results are entirely similar to SCC data (4), there can, however, be marked kinetic effects if the hydrogen entry step happens to be rate-controlling. Once dissolved, hydrogen can diffuse rapidly in most metals and particularly so in bcc metals. Another transport process also occurs which can be even faster; motion of hydrogen in dislocation cores or as Cottrell atmospheres accompanying moving dislocations. There is now increasing and persuasive evidence that dislocation transport is not only possible but that it can and does occur in iron-carbon alloys (11-15). This means that observation of environmental cracking rates which exceed the rate of hydrogen diffusion (4), do not of themselves rule out a hydrogen role in that cracking process. Hydrogen's extreme mobility in ferrous alloys at room temperature permits it to be sensitive to local stress and strain centers and to accumulate at a wide variety of locations in a microstructure, such as grain boundaries, inclusions, voids, dislocations and dislocation arrays, solute atoms, etc., as well as in solid solution. Whichever of these locations is the most sensitive to fracture will then control the magnitude of hydrogen effects, although in general all of them will accumulate hydrogen, to extents determined by their relative trapping abilities, as will be discussed. Hydrogen-induced fracture is usually thought of as brittle, and intergranular fractures are in fact common, but many materials exhibit ductile fracture (with a sharply reduced ductility) in the presence of hydrogen (8).

These viewpoints indicate how hydrogen effects can be influenced by the microstructure; of particular interest in such an approach is the (potential) control of fracture behavior by manipulating the microstructural locations for hydrogen

accumulation (5). The location most critically affected by hydrogen will form the fracture nuclei and path; this may accentuate the fracture mode which occurs in the absence of hydrogen, or it may cause a different mode to occur. Another important variable is strength level, which is generally stated to directly scale with embrittling tendency. As we have been emphasizing for some time (16), this "rule of thumb" can be a gross oversimplification which totally ignores the path dependency of environmental embrittlement. In other words, the thermomechanical processing (and composition) variables selected to achieve a given strength level can result in very different responses to hydrogen. This is graphically illustrated in reference (17), which shows the embrittling tendencies of a number of steels encompassing some 465 low to medium strength levels. While there may be a very general trend extractable from the data, the very broad scatter belies the universality of the correlation and most importantly makes it a very tenuous alloy design approach. In fact, in more controlled experiments on specific steels where thermal treatments were used to achieve low to high strengths, susceptibility was shown to be considerably more sensitive to the specific nature of the microstructure rather than to the resultant strength level (4)-(6), (18)-(20).

This brief introduction was intended to establish the philosophical base for the paper. In the following sections we will describe in some detail how hydrogen interacts with various microstructural features, denoted by the term "trapping"; how such trap interactions can modify mechanical properties, particularly fracture related ones; and finally how a full understanding of the impact and import of hydrogen can serve as a basis for identifying the reasons for a varying susceptibility and to use these to establish a framework for proper alloy design in ferrous, and very likely non-ferrous alloys. The most important factors will be shown to be the nature or type of defects that interact with hydrogen and the concept of a critical hydrogen concentration for premature embrittlement. We will examine if it is possible to either decrease the trapped hydrogen in potential crack sites or to increase the

critical valve at a given trap. Importantly, we believe it is possible to develop hydrogen-resistant steels without seriously compromising other critical mechanical properties such as strength, ductility, toughness in air and fatigue resistance.

II HYDROGEN TRAPS AND ANTI-TRAPS IN IRON-BASE ALLOYS

Definition of Trapping

By definition, a trap is a localized region where a hydrogen atom spends more time than it does on a normal interstitial lattice site. In such cases the probability of jumping into the trap should never be decreased compared to the lattice. (If it is decreased or unvarying, the heterogeneity will have a repelling or obstacle character, as will be discussed subsequently.) Further, the probability of the trapped hydrogen atom being released from the trap will also be decreased. There are in general two main reasons why in a crystal lattice jump probabilities are modified, as illustrated in Figures 2a and b:

There may exist an attractive force for the hydrogen atom in a preferred direction (Figure 2a). Forces of various origins may act on the hydrogen atom either because of its existence as a screened proton with an extra electron in the 3d band of iron, or because its small size gives it a high mobility. In such cases, the physical lattice is not modified, i.e. the average jump height is not modified from site to site, but it is easier, and hence more probable, for hydrogen to jump in the direction of the biasing force (Figure 2a) and be attracted toward its origin.

Alternatively, the physical lattice is distorted in such a manner that the average jump height is modified, thereby rendering subsequent detrapping difficult (Figure 2b). For the sake of discussion we divide traps into either attractive or physical traps, realizing that most real traps present a mixed character, with characteristics of both.

Attractive Traps

For attractive traps, the forces acting on the interstitial proton in an iron lattice are classified as follows:

Electronic force: Because hydrogen dissolves in iron by giving up its excess electron to the collective electron gas of the metal (21) (22), any defect that introduces an electron vacancy will attract hydrogen to achieve local neutrality. This will be the case for impurity atoms in iron that are located to the left of iron in the Periodic Table (22).

The most general way to characterize attractive atomic traps of electronic origin (interstitial or substitutional atoms) is by the size and magnitude of the interaction coefficient between hydrogen and a foreign atom i , ϵ_H^i (23)-(26). This is derivable from the hydrogen activity, a_H , given by:

$$a_H = \gamma_H \cdot x_H \quad (1)$$

where γ_H = activity coefficient, and x_H = atom fraction of H. γ_H can itself be expressed by:

$$\ln \gamma_H = \ln \gamma_H^0 + \sum \epsilon_H^i x_i \quad (2)$$

Now, in terms of interaction energies, when $\epsilon_H^i < 0$ an attractive force exists between the i atom and H (26). Similarly, for $\epsilon_H^i > 0$ a repulsive force exists between i and H, and for $\epsilon_H^i \approx 0$ no interaction between the two is predicted on thermodynamic grounds. While tables for ϵ_H^i exist at 1600° (24), there are few data on the evolution of ϵ_H^i with temperature, although it is expected that strongly negative or positive ϵ_H^i 's should keep the same sign as the temperature decreases (23), (25).

Forces due to stress fields: The lattice is now physically distorted (such traps also have a physical character). For example, hydrogen has "more room" in a tensile stressed region of the lattice than in a compressively stressed region and hence will migrate towards and be trapped by centers of dilation.

Forces due to a temperature gradient: Since hydrogen's solubility is increased with increasing temperatures, it will be attracted to hotter regions of the material, such as, for example, the last regions of an ingot that is solidifying.

An ideal representation of an attractive trap is given in Figure 2c. The range of the attractive force for a trap of electronic origin should be small, while for the other two cases the range should scale with the tensile or temperature gradient.

Physical Traps

All physical discontinuities in the lattice should and usually do constitute physical traps for hydrogen. Typical examples include voids, interfaces (inclusion-matrix, particle-matrix), grain boundaries, the missing plane of an edge dislocation, etc... Ideally, a purely physical trap can be visualized as in Figure 2d; the hydrogen atom sitting close to the trap is not specifically attracted, but, once trapped, it has difficulties escaping.

Mixed Traps

As mentioned earlier, it is difficult to envision traps that are purely attractive or purely physical, except perhaps a foreign substitutional atom which does not strongly perturb the lattice (e.g. Ni,Co). For most traps, both characters are probably present, since every physical distortion of the lattice is surely accompanied by an electronic disturbance. A good example of a mixed trap is that of the edge dislocation; the attractive character is due to the tensile stress field and the physical character is given by the missing lattice plane. The energy schematic of a mixed trap is shown

in Fig. 2e.

Anti-Traps: Repellers and Obstacles

Anti-traps in such systems as iron alloys are natural analogues of the attractive and physical traps defined above. The counterpart of an attractive trap is a repeller, i.e. a region of the lattice where a repulsive force exists; its energetic representation is given in Figure 2f. To repel, one or more of the following characteristics of the defect are necessary: Atoms are to the right of iron in the Periodic Table, thus introducing an excess electron in the 3d band, whereby $\epsilon_H^i > 0$; the defect introduces a compressive stress field to the lattice whether it is an interstitial or substitutional atom, a particle, inclusion, or the extra plane of an edge dislocation; or it is a region of a specimen where the hydrogen solubility is reduced.

The counterpart of a physical trap is an obstacle, i.e. a physical discontinuity of the lattice through which hydrogen has no significant mobility, as illustrated in Figure 2g. An example of such a defect that would strictly be an obstacle is an incoherent precipitate that does not dissolve hydrogen and that does not induce a local stress field.

In a similar fashion to traps, strict repellers or obstacles may be difficult to find and, in general, both characters will be present at the same time and give rise to a mixed anti-trap as shown in Figure 2h. The presence of an edge dislocation as an example of both a mixed trap and mixed anti-trap suggests that some defects may have both a trapping and anti-trapping character. This is illustrated in figures 2i through 2l, where we imagine that a hydrogen atom is moving along the direction $C \rightarrow C^1$. It is easy to visualize that this atom has to cross a mixed anti-trap region (sites 1' to 4') before being trapped (sites 5' and 7'). Other examples of mixed traps can be imagined, such as a particle with an incoherent interface that does not dissolve hydrogen. Thus the surface is physical trap while the bulk of the particle is an

obstacle.

From the above considerations, it is now apparent that hydrogen will interact (positively or negatively) with many of the defects currently found in steels; such defects range from foreign interstitial or substitutional atom to macroscopic inclusions or void. In the following sections we will examine how the traps/anti-traps characteristics of such heterogeneities can influence hydrogen diffusivity, solubility and embrittlement.

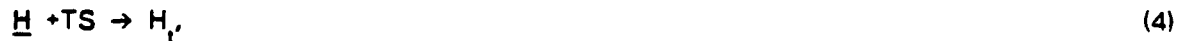
Characteristics of Traps and Anti-Traps

Reversible/Irreversible Trap Characters: In a simple case such as that of the physical trap, Figure 1d, the escape probability P_e of the H atom is given by a function of the form:

$$P_e = k_0 \exp(-E_T/kT) \quad (3)$$

where k_0 = frequency factor, E_T = trap energy depth, k = Boltzmann constant, T = absolute temperature. Since P_e has a rapidly decreasing dependency on E_T and an increasing one on temperature, at a given (low) temperature, and for a large value of E_T , the probability of escape may become very small; such traps have an irreversible character.

We consider that in general trapping reactions may be written as a first order reaction (linear trapping):



where \underline{H} = dissolved interstitial (diffusing) hydrogen atom, TS = trapping site, H_t = trapped hydrogen. The rate of trapping is given by (25):

$$dn/dt = kC(1-n) - pn, \quad (5)$$

where n = fraction of traps occupied at time t , C = hydrogen concentration in the lattice available for trapping and k and p are the capture and release constants, respectively.

In the case of a reversible trap, $p \neq 0$ and at steady state;

$$dn_s^R/dt = 0 \Rightarrow n_s^R = (kC_s/p)/(1+kC_s/p), \quad (6)$$

where n_s^R and C_s are the steady state values of n^R and C respectively and n^R is the fraction of reversible traps occupied. For a weak reversible trap (i.e. $kC/p \ll 1$) $n_s^R \simeq kC_s/p$, and at steady state an equilibrium between reversibly trapped hydrogen and diffusing hydrogen can be assumed. To the contrary, for an irreversible trap (i.e. $p = 0$), at steady state, $(dn_s^I/dt) = 0 \Rightarrow n_s^I = 1$, and the steady state value of n is now independent of C_s . In other words, an irreversible trap will saturate given sufficient time, no matter the surrounding hydrogen activity.

If saturation is defined as all trapping sites, N_T , being occupied, i.e. $n = 1$, reversible traps are not expected to saturate, since from equation (6) $n_s^R < 1$. However, if the hydrogen concentration C_s is large enough, then $n_s^R \sim 1$, and the reversible trap is thus close to saturation. However, even in this case if the trap is very reversible, i.e. if $kC/p \ll 1$, then, as shown before, $n_s^R \simeq kC_s/p \ll 1$, and the reversible trap will never saturate no matter the value of C_s . For non-saturable traps one always has $n \ll 1$, hence equation (5) can be written as:

$$\frac{dn}{dt} = kC - pn \quad (7)$$

and at steady state ($dn_s/dt = 0$), $n_s = \frac{k}{p} C_s$, which resembles the behavior of weak reversible traps, but now for the different reason that, n , is always much less than

one (as, for example, when N_T is very large). This is probably the case that exists for trapping of molecular hydrogen in voids, where

$$dn/dt = kC^2 - pn \rightarrow n_s = \frac{k}{p} C_S^2 \quad (8)$$

In such a condition, N_T , the total number of molecules that can be contained before significant void expansion occurs is very large.

Traps Evolution Characteristics: The effective trap strength should decrease with the extent of the trapped population, particularly in the case of attractive traps. For example, let the attractive electronic force be of the type:

$$F = kn\bar{e}/r^2 \quad (9)$$

where n = number of electron vacancies, \bar{e} = electronic charge, r = distance to trap.

The first trapped H atom is held with a force $F = kn\bar{e}/r^2$; if a second H atom is trapped, since it brings its own electron the trapping force will now be $F=k(n-1)\bar{e}/r^2$ for both atoms, and so on. Experimentally, this can mean that the initially trapped atom may leave as more atoms get trapped, because as the trapping strength decreases, the trap character may change from irreversible to reversible. Evidence for this sequence can be found in the literature (27), from mass spectrometry and isotopic exchange hydrogen-deuterium experiments. They found that while at a given temperature complete hydrogen degassing from a steel membrane can be accomplished, the imposition of a new D_2 flux led to additional hydrogen outgassing. This may best be interpreted as a reduction in trap strength due to trapping of additional deuterium atoms.

The above examples have suggested how the trap strength may decrease with time. In the same way, as traps fill, their trapping capacity can also decrease, although the

reverse may also happen, particularly when the heterogeneity is a physical trap. This latter process can occur if hydrogen lowers the cohesive force between host atoms (28) (29), permitting the size of a physical trap to enlarge as more hydrogen atoms trap. Such a process can occur for size ranges from the atomic scale to the nucleation of microscopic cracks, affecting such defects as grain boundaries and interfaces between an inclusion or particle and the matrix. Experimental support for this hypothesis is shown in Figure 3 (30), where the permeating flux through a steel membrane is seen to decrease when new traps (cracks) are nucleated at a critical hydrogen level. When these newly created traps (cracks) are full for either equilibrium or saturation reasons, the flux again increases. Thus, both trap capacity and strength will increase with time, but of course not without limit. Although other reasons may be found for such trapping increases, such as, for example, dislocation nucleation or surface barrier effects, the evidence cited is believed best explained by an enhanced trap capacity (30).

Heterogeneities may also be transformed from traps to anti-traps. An example of such a sequence would be an incoherent carbide particle that does not dissolve hydrogen. At first this heterogeneity is a hydrogen trap, in particular an irreversible physical interfacial trap. However, once the trap is saturated, its trapping character is lost and the particle can then behave as a volume obstacle for the diffusing hydrogen atoms.

Many of the defects identified as hydrogen traps also have the facility to move through the material, including dislocations, for which numerous examples of hydrogen transport exist (11)(12), as well as vacancies and interstitials. The effectiveness of such traps can be quite significant as they move through the matrix, interact with other traps, coalesce to form new trap types, etc. Thus, it is important to recognize that trap characteristics are not fixed properties. The evolutionary nature of traps is an additional complexity when developing the trap concept as part of a framework to use microstructural design to reduce hydrogen embrittlement.

Effect of Traps, Repellers and Obstacles on Hydrogen Diffusivity: The effect of traps on hydrogen diffusivity can be simply illustrated by reference to Figure 4. Figure 4a represents an ideal lattice without traps; in such a lattice a hydrogen atom moving in time t_d from site 1 to site N through N (successful) jumps, has an "ideal" diffusion coefficient, D_d , given by the atomic theory of diffusion:

$$D_d \equiv a^2 N / t_d, \text{ where } a = \text{jump distance.} \quad (10)$$

Figure 4b describes the situation where N_p trapping sites are now present, leaving $N - N_p$ "normal" diffusion sites. If t_a is the time taken to go from site 1 to N when traps are present, the apparent diffusion coefficient D_a is now:

$$D_a \equiv a^2 N / t_a \quad (11)$$

where t_a is considered as the sum, $t_a = t'_d + t_p$; t'_d is the time spent on the $N - N_p$ normal diffusion sites, $t'_d = a^2 (N - N_p) / D_d$ (12a)

and t_p is the time spent on the N_p trapping sites, proportional to the number of traps N_p , and inversely proportional to the escape probability, P_e , i.e.

$$t_p = K N_p / P_e \quad (12b)$$

Substituting t'_d and t_p in equation 11, and since in general $N_p \ll N$;

$$D_a = \frac{D_d}{1 + K N_p \exp(E_T / k_B T)} \quad (13)$$

where $K = k D_d / a^2 N k_o$.

Equation 13 is the most general form describing the diffusivity of hydrogen in the presence of traps, with K taking different values depending on the specific analytical

model used. Generally, and regardless of the model, it illustrates two important points: viz D_a is always less than D_d , and the decrease in hydrogen diffusivity is proportional to the trap strength and number.

A large number of models and theories have been developed to describe the effect of trapping on hydrogen diffusivity; many of these are discussed in detail elsewhere in this book (31). The physical bases for such models include equilibria between diffusing and trapped populations (32), statistical (33)-(37) and thermodynamic analyses (38), the use of electrical analogies (39) or chemical-type trapping reactions (25)(40). Recently, a quite general model based upon Boltzmann statistics has been derived by Leblond and DuBois (41), which considers not only attractive physical traps but anti-traps as well. For the case of physical traps, they derive the following relation for the apparent diffusivity:

$$D_a = \frac{D_d}{1 + (1/S_d) \sum p_k S_k} \quad (14a)$$

with S_d = solubility of hydrogen in lattice sites; P_k = volume proportion of sites of type k ; S_k = solubility of hydrogen in k type sites. The form of (14a) is quite similar to (13). The success of this or any other model ultimately rests with its successful application to experiments. However, great care must be taken when applying data because of the difficulty of identifying the precise trap responsible for the observed effect and because other unrecognized phenomena may affect hydrogen diffusivity (e.g. surface effects, anti-traps). For example, an alternative scenario to trapping is when a diffusing hydrogen atom is forced to go around a repeller or an obstacle; its diffusing path is thus lengthened, and again, the apparent diffusivity will be lower, as illustrated by Figure 5, where the general form of the apparent diffusion coefficient is now given by:

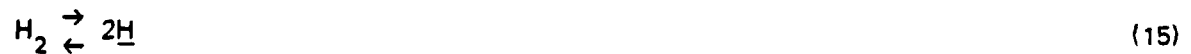
$$D_a = \frac{D_d}{1 + ka^2} \quad (14b)$$

where k is a constant ($k = 1/L^2$ in Figure 5, with $L =$ diffusion length), and a is the effective barrier dimension of the anti-trap. More generally, "a" is the dimensional equivalent of the physical obstacle perpendicular to the hydrogen flux, with an additional value due to the range of the repulsive stress if the barrier also acts as a repeller.

Very few models to date have taken anti-traps into account when trying to describe anomalous effects of hydrogen diffusion in steels, other than the most recent one cited (41) where it was found that while for this case D_a had a form similar to that given by equation (14b), the influence of the anti-traps was only significant at high volume fractions. Notwithstanding the lack of specific models, experimental evidence for the decrease in hydrogen diffusivity due to anti-traps abounds in the literature, although the effect was not generally recognized as such. Figure 6 gives such examples for both atomic traps and anti-traps. Thus trapping elements, like Mn, Ti, Zr etc. where $\epsilon_H^i < 0$ and repeller elements like Co, Pd and Ni where $\epsilon_H^i > 0$ both lower D_a .

Magnetic techniques can be used to more precisely distinguish traps from anti-traps (49); it was found that Me-H complexes form with Ti and Zr additions (traps), while none are detected with Co, Pd and Ni (the results for Ni are somewhat contradictory, as shown in Table I).

Effect of traps, repellers and obstacles on hydrogen solubility: For the case where alloying elements, "i", have been added to a ferrous material subjected to a constant external hydrogen pressure, p_{H_2} , the following equilibrium holds:



where the equilibrium constant is defined by:

$$k = a_{\underline{H}}^2 / p_{H_2} \quad (16)$$

where $a_{\underline{H}}$ is the activity of dissolved hydrogen \underline{H} . If p_{H_2} is taken to be constant then from equations (1) and (2) we obtain:

$$a_{\underline{H}} = \left(\gamma_{\underline{H}} \right) \left(x_{\underline{H}} \right) = \gamma_{\underline{H}}^0 \exp \left(\sum \epsilon_{\underline{H}^i}^i x_i \right). \quad x_{\underline{H}} = K \sqrt{p_{H_2}} = \text{constant} \quad (17)$$

which of course is simply Sievert's law.

Now, if the alloying elements added are atomic traps, i.e. $\epsilon_{\underline{H}^i}^i < 0$, any increase in X_i will result in an increase in $x_{\underline{H}}$ to maintain the term $\left(\sum \epsilon_{\underline{H}^i}^i x_i \right) x_{\underline{H}}$ constant. This leads to the prediction that hydrogen solubility is increased with the addition of attractive traps, a result that would also be obtained if physical traps were considered. The total quantity of hydrogen increases both by the amount of hydrogen in traps plus a supplementary amount of hydrogen in the lattice due to the presence of any attractive traps and its resultant effect on activity of hydrogen in solution. This prediction is independent of the specific model. For example, using McNabb-Foster equations at steady state (equations (5) to (8)), the total quantity of hydrogen Q_s is given by:

$$Q_s^R = C_s + n_s N_T = C_s \left[1 + \frac{k/p N_T}{1+k/p C_s} \right] \quad (18)$$

$$\text{and } Q_s^i = C_s + N_T$$

for reversible (Q_s^R) and irreversible traps (Q_s^i), respectively. Thus, hydrogen's total quantity increases with trap concentration (as compared to a trap free material subjected to a same external hydrogen activity) in a manner dependent on both trap number and their characteristics. Figures 7a and b show high and room temperature data demonstrating that hydrogen solubility is increased with the addition of those alloying elements suspected as acting as hydrogen atomic traps (50) (51), e.g. Nb, Mn,

Cr and Ni.

Using similar reasoning as for traps, described by equation (18), it can be seen that any increase in the concentration, X_i , of alloying elements "i" having a positive ϵ_{H}^i (atomic repellers), will now result in a decrease of hydrogen solubility, X_H , to keep a_H constant. This prediction is intuitively reasonable since the more numerous the obstacles and repellers, the less "room" available for hydrogen.

As was the case for the effect of anti-traps on hydrogen diffusivity, only the model of Leblond and Dubois (41) attempts to theoretically describe how these features effect solubility. They have developed a predictive relation with the same form as the one for the effect of anti-traps (Eqn. 14b) on diffusivity, but now with a reducing factor in the equation. For the case of atomic repellers, Figures 7a) and 7b) illustrate that solubility is indeed lowered by addition of elements with a positive ϵ_{H}^i , e.g. Cu, Co, Sn, Ge, Al, B, C, S, P.

From the above it is clear that any analyses based on diffusivity measurements alone cannot discriminate between the different forms of traps present, since both traps and anti-traps have the same delaying effect. Thus many analyses found in the literature where permeation curves are fitted with a given set of parameters relying only on a trapping model are probably incomplete. Only in those analyses where a pure trapping element is varied (42) can current trap models be adequately interpreted, since in such cases anti-traps effects may then be considered constant. In fact, distinguishing between traps and anti-traps effects by standard permeation techniques is only possible if temperature measurements are also performed, since repellers and obstacles are usually insensitive to temperature changes, while traps may exhibit specific temperatures above which they become much more reversible. The Arrhenius plot for traps should exhibit a larger break for traps than for anti-traps, as schematically illustrated in Figure 8. It is best to always perform permeability measurements, since the permeability, P , is the product of the

diffusivity and the solubility of hydrogen, and thus in the case of a material with an increasing amount of an anti-trap, P should decrease, while for a trap P could either increase or decrease, depending on whether the effect on solubility or on diffusivity is greatest.

Effect of dislocations on hydrogen transport: We have stated before that hydrogen can be trapped at mobile defects such as dislocations, vacancies, voids and interstitial atoms. In contrast to the usual delaying effect induced by such traps when they are static, an opposing "accelerating" effect may be initiated whenever such traps are put into motion. Several models in the literature have examined such situations (13),(52) for the case of transport of hydrogen by dislocation, which are expected to differ from interstitial diffusion in the following ways:

Transport by dislocations will be faster than for lattice diffusion, up to 10^4 faster for a standard room temperature tensile experiment.

Dislocation lines will transport more hydrogen than the same length of a normal diffusion front. Estimates (13), (52) give 10^3 times more hydrogen being transported by dislocations than by the lattice (up to 10^3 atoms H/cm).

The interaction of hydrogen trapped on moving dislocations with any encountered defects will be much different than the interaction with hydrogen on lattice sites, since the binding energy to a dislocation is considerably larger than to a lattice site. In other words, it will be more difficult for an encountered defect to take hydrogen from a dislocation than from a lattice site. In essence, this means that moving dislocations may act as a sink or source of hydrogen depending on the trapping strength of the encountered defect (52).

Only that part of the lattice swept by dislocations will be involved, as opposed to interstitial diffusion, which invariably encompasses the whole volume of the material.

As previously cited, a number of experimental results have strongly suggested the existence of a dislocation transport mechanism. For example, the absorption of tritium in the plastically strained region of a tensile specimen subjected to an external tritium atmosphere was greater than in the unstrained exposed regions outside the gage length (11). Similarly, large amounts of hydrogen outgassing in

charged specimens has been strongly correlated to the onset of plasticity (11) (27).

Recently much more compelling evidence has been found in both polycrystalline (12) and single crystal iron (14) for dislocation transport of hydrogen. Straining permeation tests clearly revealed the dual nature of dislocations as traps and as transporters of hydrogen. The former effect dominates at low strains and for crystals oriented for multiple slip when the generation of new dislocations is very high so that immobile dislocation networks can more easily form. For single slip orientations, on the other hand, both edge and screw dislocations can carry significant quantities of hydrogen at room temperature as revealed by discontinuous changes in the hydrogen flux, due to hydrogen egress from the surfaces intersected by active slip bands. The combination of enhanced hydrogen trapping, resulting perhaps in void formation at dense tangles, with enhanced transport to other potential fracture centers must be taken into account in any successful unified description of hydrogen embrittlement.

Summary of Trap and Anti-Trap Classification

Table 1 provides in summary form examples of defects that should act as traps, repellers or obstacles. Most generally, an element located to the left of iron in the Periodic Table exhibits a negative ϵ_H^i , while elements to the right of iron have a positive ϵ_H^i . Two exceptions are molybdenum and nickel. For Ni, the most recent results on ϵ_H^i (24) gives a very slightly negative ϵ_H^{Ni} (-0.05), while older data (50) gave it a null value. For molybdenum, contradictory information also exists; ϵ_H^{Mo} given as being negative (50) or positive (24). Since both elements are not too far from iron in terms of electronic outer shells ($4d^5$ for Mo, $3d^8$ for Ni instead of $3d^6$ for iron), other effects such as ionic radii may be important. Contradictory ϵ_H^i values also exist for oxygen; however, the ϵ_H^O value for the most recent reference (24) is much greater than that of the older one (50) (-12 instead of 1.1), and is probably more realistic.

Surprisingly, some elements that were (indirectly) suspected as hydrogen traps appear to be promising repellers; such is the case for C and N (57). In the same way, the slightly positive value of $\epsilon_{\text{H}}^{\text{H}}$ of 1.0 should rule out the formation of H-H pairs in iron.¹

Finally, it must be emphasized that these considerations are valid for lone atoms in a perfect iron matrix. It is difficult to assess, for example, the repelling role of the metalloids in Table I (P, S, As, Sb) when these preferentially segregate on grain boundaries.

III ROLE OF MICROSTRUCTURE ON HYDROGEN RELATED PROPERTIES

In the previous section we have examined in detail the many different ways hydrogen can interact with specific types of microstructural heterogeneities, which themselves are describable by their relative trapping or anti-trapping behaviors. In this section we will briefly summarize how such interactions can and often do affect microscopic and macroscopic mechanical properties. Much more detailed descriptions are the subjects of other chapters in the book.

Effect of hydrogen on dislocation and precipitate behavior in iron and steel. Besides the previous demonstration of the trapping abilities of dislocations of various types and the relative efficiencies of edge, screw and mixed dislocations to transport hydrogen, there is the complementary question of whether hydrogen can affect the nature of the dislocation population, either through enhanced transport of one type, by changes in stacking fault energies or by affecting dislocation-dislocation interactions. Similarly, it is important to examine if hydrogen directly affects precipitation or inclusion character, such as the strain for coherency loss, interfacial strength and the like. These factors are important in the present context since we

¹This would also be in agreement with the fact that the electronic force between H atoms should be repulsive, since each atom introduces an excess electron.

must know the hydrogen-related stability of proposed microstructural modifications.

There is little convincing evidence to support significant hydrogen-induced changes for either case, dislocations or precipitates, although there is more circumstantial support for a direct effect in dislocations. For example, the observations in hydrogen containing materials, ranging from high purity iron to high strength steels, of a lower friction stress and increased Petch slope (59), lower yield strengths and higher work hardening rates (60) and a significant increase in strain localization (61), are all suggestive of fundamental changes in the ways dislocations move and interact with each other and with other heterogeneities. However, such changes have never been directly observed and this is clearly an important area for future study.

So far as observed direct changes in precipitate or inclusion behavior, there are even fewer results than above. One of the successful attempts to assess such effect was by Garber et al (62), who found that hydrogen did not measurably change the local stress for void nucleation at spheroidized carbides. However, considering the surface active nature of hydrogen, it would be surprising if hydrogen would be unable to influence the kinetics of coarsening, strain induced changes at precipitate interfaces etc. in some systems. The numerous observations of a synergistic effect between hydrogen and temper embrittlement (63) as well as other observations of hydrogen-solute interactions lends credibility to the suggestion.

The occurrence of direct hydrogen-induced changes on the microstructure can have a serious impact on the effect that has been more normally considered; viz. changes in local or global fracture criteria, particularly since the emphasis has been shifting towards a greater contribution of hydrogen induced plasticity effects on fracture (59), even when the fracture appears "brittle" in appearance. Thus, the ability of hydrogen, in some way, to modify how strain is concentrated could have profound effects on any number of events which act as a precursor to final fracture. For example, changes in strain accommodation at interfacial boundaries, such as grain or

lath boundaries or matrix particle interfaces, can lead to premature failure, strain localization changes can promote slip plane cracking or modify events within the plastic zone (61). More generally, the way in which hydrogen interacts with precipitate or other particles located on or near different structural features can in many cases directly control the type of hydrogen-induced fracture. These sequences are schematically illustrated in Fig. 9 (4), emphasizing the possible roles of hydrogen in nucleating fracture (an event which of course can differ in scale and type from propagation). The figure describes, in turn, particle induced micro-void coalescence (MVC); cleavage triggered by a combination of inclusion cracking and the satisfaction of a local stress-distance criteria, quasi-cleavage related to a highly localized ductile fracture related to either MVC or inclusion cracking; and finally intergranular or interfacial fracture triggered by cracking or void growth of a particle.

The importance of presenting this figure is that it unifies a viewpoint discussed most completely by Thompson and Bernstein (4), who have emphasized the multiple ways by which hydrogen can affect the fracture process. They have emphasized that while on a local scale (perhaps of atomic dimensions) the fracture can be highly brittle, most often the more dominant fractographic features are plasticity related where extent and degree of localization scales with macroscopic ductility parameters. The most reasonable and most useful viewpoint is that hydrogen can affect fracture on both scales, with the relative importance and proportions of each being controlled by microstructural features. Specifically then, the observed fracture mode will be determined by such factors as the partitioning of hydrogen to potential fracture nuclei or innocuous traps, the ease of local brittle fracture or local shear, and, most importantly for propagation, the continuity of the embrittled phase, or equivalently, the ability of local fracture criteria to be continuously attained. This multiplicity of hydrogen-related processes not surprisingly leads to many fractograph forms of hydrogen embrittlement and, importantly, to the oft unrecognized fact that there need not be a direct correlation between the extent of embrittlement and how brittle the

fracture appears.

These sections have emphasized and described in some detail the causal interactions between microstructural and hydrogen embrittlement. To better appreciate this approach, the next section will describe a broad number of examples where microstructural manipulations, which affect trapping or anti-trapping and/or the ease of fracture initiation and growth, can be and have been used to reduce the extent of hydrogen embrittlement in a number of ferrous alloys, ranging from low strength microstructurally simple systems to high strength microstructurally complex alloys.

IV ROLE OF MICROSTRUCTURE IN THE DESIGN OF HYDROGEN-RESISTANT ALLOYS

As we have discussed in the previous sections, hydrogen initiation or assisted cracking or fracture may be considered to be fundamentally related to a critical amount (C_K) of trapped hydrogen (C_H) on any given trapping defect. This will serve as a major focus in developing the underlying philosophy of alloy design through microstructural manipulation and control. Following a number of examples for each variable of importance, more general and successful examples will be given.

Any correct design of a hydrogen resisting material should try to both increase the C_K value of those traps that are potential crack nucleation sites (i.e. those that otherwise have low C_K values), and to lower the amount of trapped hydrogen on these sites, C_H . As a first step Figure 10 illustrates schematically both the important parameters acting on C_H and C_K , as well as the most important heterogeneities that can and do act as hydrogen traps or antitraps. As such, it serves as a logical extension of the parameteric parameters first introduced in Figure 1. The important C_K parameters include defect shape, size and distribution, degree of coherency, segregation, as well as the neighboring microstructure; each of these are in turn affected by and sensitive to chemical composition and thermomechanical treatments.

The important C_H parameters are time of exposure to the environment, absorption kinetics (related to surface state), hydrogen transport mode, the hydrogen external and internal activity and the presence of other traps. The parameters common to both C_K and C_H are temperature and applied stress. In order to continue our focus on microstructure, we will limit the discussion to those parameters related to the material itself. Thus the possible beneficial roles of surface effects (i.e. hydrogen barriers) or external hydrogen activity (i.e. inhibitors) will not be considered; use of these parameters have been described elsewhere (5).

Design of Hydrogen Resisting Steels through an Increase in C_K : shape as a control parameter connotes such features as inclusions (e.g. sulfides, oxides, oxisulfides), particles (e.g. carbides, nitrides, carbonitrides), and even grain boundaries in some highly textured materials. It can be most important role since it often determines the hydrogen pressure that can be reached at an interface, as suggested by Figure 11 (64), as well as modifying the local stress states (65) and resultant diffusivity of hydrogen to the defect (66). Considerations of the control factors for each of these (5) predicts that elongated shaped particles with sharp extremities exhibit lowest C_K values in that cracks will start from sharp extremities and, further, that such cracks will initiate at lower trapped hydrogen concentrations; Figure 12 provides an illustration of such a hydrogen sulfide induced crack at the extremity of an elongated MnS particle.

Hence, round shaped second phase particles are desirable, which are achievable by several means: In the case of manganese sulfides inclusions, which are soft at normal working temperatures, the elongated shape results from rolling or forging operations. Calcium or rare earth (RE) additions results either in MnS alloyed with the Ca or RE, which initiate or grow around Ca or RE oxides; all of these inclusions are harder than simple MnS and hence less deformable. There does exist, however, a critical amount of the addition, since too small an addition will be insufficient to harden the inclusions, while too large will result in cluster type precipitation of RE-

Ca-oxisulfides that can themselves be detrimental to hydrogen resistance. Figure 13 illustrates such a typical Ca-RE treatment for shape control which also takes into account oxygen, manganese and sulfur content (5). Another approach to shape control is to use other particles, which precipitate early in the melt and which serve as both MnS nucleation sites and hardening centers. This is the case for titanium nitride around which MnS may grow (67). Perhaps the best method is to lower the sulfur content below 2×10^{-3} wt% which promotes the formation of round MnS particles, as illustrated in Figure 14, taken from a statistical analysis of more than forty C-Mn steels (5). Such low sulfur values are possible through vacuum degassing or ladle refining steelmaking techniques. Finally, in the case of such particles as Fe_3C and carbonitrides, round particles may be obtained using specific thermomechanical treatments. It will be shown later that such spheroidal carbide structures can provide excellent hydrogen resistance.

Size, another control parameter, concerns dimensions of defects ranging from inclusions, particles and voids to the grains themselves. In the case of the first three, large sizes are detrimental because of the resulting higher probabilities to find such inclusions, particles or voids located in low C_x zones. For instance, a large (and even round) inclusion will have a higher probability to cut or lie along grain boundaries; hence cracks can then follow the more susceptible grain boundary, contrary to the case of a smaller inclusion restricted to the matrix. Figure 15 illustrates this point with grain boundary cracks branching from a large round oxisulfide. While small inclusion sizes may be obtained by providing more numerous nucleation sites to inclusions in the liquid melt (67), the best approach still is to decrease the metalloidal content (5), as illustrated in Figure 16 for MnS inclusions. Decreasing from sulfur 14×10^{-3} wt % to 10^{-3} wt % reduces the MnS size from [7 by 2] μ^2 to less than [2 by 2] μ^2 . A large grain size is also detrimental since the associated lower grain boundary area provides fewer trapping sites and thus the probability increases that the concentration of hydrogen trapped on grain boundaries

can reach its C_K value faster.

Generally speaking, a heterogeneous distribution of particles will favor local high hydrogen concentrations with concomitant deleterious effects such as localized decohesion. Typical examples include MnS stringers in segregated zones, oxide stringers, and preferential carbide precipitations on grain boundaries. For the first of these a more homogeneous MnS distribution can be obtained, as discussed previously, by providing numerous nucleation sites in the liquid melt (67), by alloying the sulfides with inclusions that precipitate earlier, such as Ca and RE oxides, by adopting an ingot shape that reduces segregation (e.g. ingots with a larger diameter at the top, hollowed ingots or continuous casting techniques) by stirring the liquid melt, or by reducing the sulfur content (5).

Segregation of impurities is essentially an interface problem, including but not limited to the boundaries between inclusion/particle and the matrix, or grain boundaries. Some segregating impurities, such as metalloids (phosphorous, antimony, arsenic), are known to reduce the cohesive strength of the interface, which may in and of itself be cumulative to any direct deleterious effects of hydrogen and such segregation should be avoided. Particularly prone to such segregating effects are steels containing Ni, Cr, Mo or austenitic steels (e.g. sensitized 304L) that exhibit temper embrittlement to which hydrogen degradation effects may be additive and are certainly synergistic. However, even more common C-Mn steels may also have segregated zones, due to poor steelmaking practice, allowing metalloids to concentrate. Besides reducing interface or boundary cohesive strength, the segregated impurities may also be catalytic recombination poisons, thereby promoting hydrogen absorption under cathodic polarization conditions (68). Table II (5) summarizes a number of approaches which may provide useful directions in reducing segregation.

Another important control parameter is the degree of precipitate coherency. In

general, incoherent interfaces can both offer less cohesive strength as well as provide more "room" for hydrogen and segregating impurities to be trapped. Such interfaces may be minimized through appropriate thermomechanical treatments, but incoherent inclusions or high angle grain boundaries are difficult to avoid. In such cases it may be possible to use selective segregating elements that themselves increase grain boundary cohesive strength.

Finally, and more globally, every defect susceptible to hydrogen cracking resides in a microstructural environment that will ultimately determine the defect's C_K value. The response of this population depends on composition, thermomechanical history, and on the steelmaking process itself.

By chemical composition, we mean all elements deliberately present alone and in combination in the nominal composition of a given steel. Although it has been stressed a number of times (4), the synergistic influences of different impurities have not been systematically studied. For example, when looking at the role of a particular element on hydrogen embrittlement susceptibility, it would seem logical to add this element in varying amounts while keeping the base composition constant. This is rarely done, and when it is, it is not obvious whether the added element is acting as a free atom or in a combined form. Nevertheless, some broad trends can be drawn, as summarized in Table III (5), in agreement with previous assessments (4). It appears that manganese is generally detrimental, while additions of silicon, vanadium, niobium, cobalt, palladium are generally beneficial. In most realistic cases the effect of most solutes is mixed, sometimes exhibiting a critical content above or below which hydrogen embrittlement increases; such seems to be the case for nickel and molybdenum (4)(6). It is thus probable that each solute addition can have a complex interaction with the other alloying elements, and that such synergistic effects are particular to each steel. For example, the role of solutes on specific and different microstructural development can be varying, leading to increases or decreases of matrix or interface cohesive strength, of stacking fault energies, in

dislocation mobility and in the resistance to crack initiation, propagation and arrest. We will also see that C_H can be influenced in a seemingly varying manner by chemical composition. Despite these apparently insurmountable complexities, there have been a number of successful examples of compositional control to reduce the tendency for embrittlement, as will be discussed. However, what is still lacking is a more systematic and confident understanding of when to use a particular element or a combination of elements.

As with chemical composition, the particular microstructure obtained through a particular thermomechanical treatment does not provide a unique C_K (or C_H) dependency. For example, two steels may have apparently identical microstructures after identical treatments, and yet widely differ in hydrogen susceptibility, due perhaps to slight differences in impurities (such as S or P) or other traps, or to subtle changes in thermomechanical treatments. Nevertheless, this is a more controllable and successful parameter and from previous considerations in this chapter and from results to be shortly discussed (69)-(70), a "successful" microstructure can be described. As an example, a distribution of small carbides in a stress-relieved matrix (e.g. quenched and tempered microstructure) should resist hydrogen embrittlement better than a structure with larger and more angular carbides (e.g. normalized structures) or a structure with high residual stresses (i.e. untempered martensite). These predictions and their limitations are discussed in more detail in references (4)-(6).

Finally, the specifics of the steelmaking and ingot pouring technique employed can also influence microstructure homogeneity. In particular, one can obtain macro-segregation where now dimensionally large zones exist where both chemical composition and microstructure will widely vary. To avoid such problems, the following steps may be useful: Reduce the concentration of segregating elements like manganese, silicon and metalloids (104), thermally treat to ensure complete transformation of the austenite (105), and use properly shaped ingots such as those

with larger tops than bottoms (105)-(106).

Practical examples of the influence of C_k on embrittlement: The above discussion has considered "good" and "bad" characteristics of trapping defects and neighboring microstructure, based on conceptual developments; there are now a growing number of concrete examples that such approaches can be fruitful: Consider first the deleterious role of MnS. For a number of experimental C-Mn steels tested with no applied stress in the NACE sulfide stress cracking medium, very little, if any, cracking occurs below a sulfur content of 2×10^{-3} wt %. Even when an external stress is applied, the beneficial behavior is retained for testing in either the transverse or longitudinal directions (107). To the contrary, if such steels have a higher sulfur content and hence elongated sulfides, they are now very sensitive to the direction of the applied stress, with very low resistance to sulfide stress cracking in the short transverse direction (i.e. the stress perpendicular to the long axis of the elongated sulfides). A similar beneficial effect of low sulfur and low phosphorous, i.e. of favorable inclusion characteristics, has also been found in higher alloyed steels similar to AISI 4140, as illustrated in Figure 17; a reduction of sulfur content from 21×10^{-3} wt % to 5×10^{-3} wt % leads to a gain of 100 MPa in threshold SSC behavior .

Oxides inclusions can also degrade hydrogen performance, particularly if they are present in large sizes and with a heterogeneous distribution. This is illustrated in Figure 18, which shows an increase in F% (a "fragility" or embrittlement index, as defined in the Figure) with the steel oxygen (oxide) content.

The role of segregation in commercial steels can also be evaluated by hydrogen embrittlement testing at various locations across the thickness of a plate, since segregated zones are usually found in the center of a steel plate. A study of high pressure hydrogen rupture resistance on 30 different heats of steels revealed that most specimens taken at mid-thickness exhibited a higher susceptibility (as

evidenced by a higher bursting pressure in helium as opposed to hydrogen gas), which can be traced back to the presence of segregated zones (108).

As another practical example, Figure 19 shows results for two laboratory heats of forged C-Mn steels hydrogen tested after various thermomechanical treatments; again an increase in the fragility index (F%) denotes an increasing susceptibility. The two steels simulate a composition akin to a segregated zone (more C, Mn, Si, S and P) and the base composition with "normal" levels of the cited elements. As the Figure shows, the best performance is found for a quenched and tempered treatment, followed by normalized and tempered, with the most pronounced hydrogen susceptibility found in the "segregated" steel. Apparently, a normalizing treatment is not sufficient to reduce the segregated zone structure. We will shortly describe an even more impressive improvement of properties due to heat treatment (70).

Design of Hydrogen Resisting Steels through a Decrease of C_H : As with our analysis of C_K we will restrict our considerations to those parameters related to the material itself; the role of surface barriers, inhibitors, degassing, transport mode, etc. on C_H will not be taken into account. The interested reader can refer to the considerable literature on this subject (see, for example, (5),(89)). Further, since many of the approaches are similar to those used for reducing C_K , we will not go into the same level of detail for C_H . The main goal is to identify heterogeneities (either traps or anti-traps) which can prevent hydrogen from accumulating on dangerous trapping defects. In other words, we want to reduce C_H on low C_K defects.

Concerning traps, the desirable characteristics are the following: A high critical concentration of hydrogen is required to initiate premature failure, so that the added traps can better resist crack initiation. The best candidates for this appear to be atomic traps or rounded small particles; a sufficient quantity of traps in order to delay the time for the saturation of beneficial traps; an irreversible character to the traps since recent models (109)-(111) have shown that reversible traps may act as

hydrogen sources and release hydrogen that is then available elsewhere for crack initiation; and finally, a homogeneous distribution of traps is important to avoid local accumulations of hydrogen.

Concerning anti-traps, which ideally should also be used to decrease C_H (by lowering hydrogen solubility) and hydrogen diffusivity, the desirable characteristics should be a very strong repelling character (which will be proportional to the anti-trap size, number and repelling strength) and a homogeneous distribution.

Practical Examples of the Influence of C_H Parameters Characteristics: Traps corresponding to the descriptions given above are such atomic elements as Sc, La, Ca, Ta, Nd, Hf, Y (54) or carbonitrides with elements such as V, Zr, Ti, Nb, B. A survey of literature data on the use of traps as a way to reduce hydrogen embrittlement is given in Table IV and a typical result is shown on Figure 20, where the NACE H_2S delayed rupture test has been performed on a 4140 type steel and on one where 0.15% V was also added. With identical yield strengths of about 790 MPa, the trap addition of fine VC carbides leads to a 200 MPa improvement in the threshold stress for sulfide stress cracking. In the synthesis section we will present further evidence of how traps can improve performance.

It should be reiterated that the use of traps should be done cautiously since this solution may only be temporary, until the traps saturate. However, the delay and the associated improvement offered by traps may nevertheless be considerable, particularly for those applications which do not have an unlimited hydrogen source, such as welding. Care should also be taken to ensure that the addition of traps do not lead to a deterioration of mechanical properties or that thermomechanical treatments do not modify a beneficial trap distribution and make it noxious.

In the case of anti-traps, it is of interest that many elements identified as repellors/obstacles have been recognized as beneficial additions, as shown in Tables I

and IV. These include palladium, cobalt, aluminum, silicon, gold, platinum, silver and sometimes copper. On the other hand, other elements, suspected as repellers, have been shown to be detrimental, such as carbon and the metalloids S, P, As, Sb. A cautionary note is again required as the above classification for repellers may only be valid for individual atoms in the matrix, often not the case for elements, which either form particles (e.g. carbon), inclusions (e.g. sulfur), or segregate to grain boundaries and interfaces (e.g. P, As, Sb). Hence, beneficial results from such repelling elements may rarely exist in steels, and the deleterious role of these may result from factors other than anti-trapping.

Synthesis

The developments described in this chapter have been intended to demonstrate that the role of specific microstructural variables or the extent of hydrogen embrittlement can not only be identified, but that identified and responsible features can be manipulated to improve performance using the dual fundamental concepts of the critical amount of hydrogen needed to initiate premature failure, C_K , and the trapping capacity of a given heterogeneity, C_H . It is apparent that such an approach is a viable one which can be exploited in model and commercial steels to improve performance and we have given some very specific examples where such specific improvements have been demonstrated. By way of a conclusion, we wish to use two further examples to demonstrate that not only is microstructural manipulation possible, but that the improvements in environmental embrittlement can be dramatic without a concomitant penalty in strength or fracture toughness. The examples selected are a model HSLA steel containing titanium (69)(71) and two commercial high strength steels, HY130 and 300M. (70)

HSLA Steel: This alloy contains 0.064C, 1.37Mn and 0.22Ti as the primary additions, and a high temperature quench and subsequent ageing was used to produce an acicular ferritic microstructure of fairly constant strength level with a varying

distribution of Fe_3C and TiC precipitates. Tensile tests on cathodically charged samples were used to monitor hydrogen sensitivity and correlated with hydrogen permeability studies to relate changes in susceptibility to the nature and degree of hydrogen traps (69). These results are summarized in Figures 21 and 22. The former compares the hydrogen free reduction in area to the value in specimens containing 2-5ppm (by wt) of internal hydrogen. Ageing to 500°C improves hydrogen performance significantly and this has been associated with the presence of coherent TiC particles which act as strong traps (69). The degradation at higher temperature manifested by intergranular fracture results from a synergistic interaction between hydrogen and temper embrittlement due to P segregation to prior austenite grain boundaries (69), a phenomenon beyond the scope of these considerations. Figure 22 shows that as the trap strength increases, as revealed by an increasing difference between the effective diffusivity measured from the first and second permeation transient (89), hydrogen performance improves at least until the intergranular embrittlement at ageing temperatures above 500°C intervenes. These results have been modelled and interpreted (69) as strong evidence for the beneficial value of strong hydrogen traps. The great value is that the solute additions and necessary thermal processing are compatible with procedures commonly used for conventional HSLA steels.

300 M and HY130 Steels: These are low alloy high strength steels; Table V shows their composition along with the heat treatment employed and the microstructures obtained. Hydrogen performance was evaluated on double cantilever beam fracture mechanics specimens in artificial sea water with zinc coupling to the specimen to increase the hydrogen activity. Figure 23 shows the stress intensity dependence of crack velocity for a number of microstructural conditions selected for similar yield strength and K_{Ic} levels (70). It is graphically clear that dramatic improvement in both the threshold stress intensity and the stage II crack velocity are possible by microstructural manipulation. While the precise reasons for such improvements are

still being studied, the origin appears to rest at least in part with the relative distribution and stability of retained austenite, a heterogeneity which is both a sink and a trap for hydrogen.

The last two examples provide compelling, if as yet incomplete, evidence for the critical role of microstructure on the extent of hydrogen embrittlement in ferrous alloys, and supports the premise of this chapter that improved alloy design is clearly possible. It would appear appropriate to summarize the current state as one where the framework for a fundamental approach to the development of improved alloys exists, but where considerable need for additional analysis and modelling remains. Optimistically, when this is accomplished, it will be easier to evaluate the applicability of current hydrogen embrittlement theories or, if necessary, to develop new ones.

Acknowledgement

We are pleased to acknowledge the financial support of the Office of Naval Research (IMB) and Creusot-Loire Research Center (GMP) and the many useful discussions with Prof. A.W. Thompson. We also wish to thank a number of graduate students at Carnegie-Mellon University, in particular R. Kerr and Dr. M.F. Stevens for permission to present some of their data prior to other publication.

References

1. W.H. Johnson, Proc. Royal Soc. (1875) no. 158 p. 168.
2. Hydrogen Metals (I.M. Bernstein and A.W. Thompson eds.) ASM, Metals Park, Ohio (1974).
3. Effect of Hydrogen on Behavior of Materials (A.W. Thompson and I.M. Bernstein eds.) TMS, Warrendale, PA (1976).
4. A.W. Thompson and I.M. Bernstein, in Advances in Corrosion Science and Technology, Vol. 7 (R.W. Staehle and M. Fontana, Eds.), (1980), p. 53.
5. G.N. Pressouyre, in Current Solutions to Hydrogen Problems in Steels, (C.G. Interrante and G.N. Pressouyre, eds.) ASM, Metals Park, Ohio (1982), p.18.
6. I.M. Bernstein and A.W. Thompson, in Alloy and Microstructural Design (J.K. Tien and G. Ansell, eds.), Academic Press (1976), p. 269.
7. I.M. Bernstein and A.W. Thompson, Effect of Metallurgical Variables on Environmental Fracture of Steels, Internat. Met. Reviews, 21 (1976), p. 269.
8. A.W. Thompson in Environment-Sensitive Fracture of Engineering Materials (Z.A. Foroulis ed.) TMS, Warrendale, PA (1979), p. 18.
9. Hydrogen Effects in Metals (I.M. Bernstein and A.W. Thompson, eds.), TMS, Warrendale, PA (1981).
10. Hydrogen and Materials, Proc. 3rd Int'l Congress, Paris (1981).
11. J.A. Donovan, Met. Trans., 7A (1976), p. 1677.
12. C. Hwang and I.M. Bernstein in Hydrogen and Materials, Proc. 3rd Int'l Congress (P. Azoved), Paris (1982), p. 1845.
13. J.K. Tien, A.W. Thompson, I.M. Bernstein and R.K. Richards, Met. Trans., 7A (1976), p. 821.
14. C. Hwang and I.M. Bernstein, Scripta Met., 17 (1983).
15. P. Bastien and P. Azou, C.R. Acad. Sci. Paris, 232 (1951) p. 1845.
16. A.W. Thompson and I.M. Bernstein in Metallurgical Treatises (J.K. Tien and J. Elliott, eds.) TMS, Warrendale, PA (1981), p. 589.
17. C. Zmudsinki, L. Bretin and M. Toitot in Hydrogen in Metals (Paris) 3, paper 6A-2 (1977).
18. I.M. Bernstein, A.W. Thompson, F. Gutierrez-Solana and L. Christodoulou

in Current Solutions to Hydrogen Problems in Steels
(C.G. Interrante and G.M. Pressouyre, eds.), ASM (1982), p. 259.

19. A.W. Thompson and I.M. Bernstein in Hydrogen Effects in Metals
(I.M. Bernstein and A.W. Thompson, eds.), TMS, Warrendale, PA
(1981), p. 291.
20. M.F. Stevens, I.M. Bernstein and W.A. McInteer, ibid p. 361.
21. R.A. Oriani, Proceedings of Conf. on Fundamental Aspects of Stress
Corrosion Cracking, (R.W. Staehle et al., eds.) NACE (1967), p. 212.
22. J. Friedel, Ber. Bunsenges. Ges., (1972), 76 No. 8, p. 828.
23. C.H.P. Lupis and J.F. Elliott, Acta Met., 14 (1966), p. 529; Acta Met.,
15 (1967), p. 265.
24. G.K. Sigworth and J.F. Elliott, Met. Sci. J., 8 (1974), p. 298.
25. A. McNabb and P.K. Foster, Trans. TMS-AIME, 227 (1963), p. 618.
26. H. Nabuchi, H. Nakao, Trans. ISIJ, 23 (1983), p. 504.
27. P. Tison, C. Pirrovani, J.P. Fidelle, Congress on Hydrogen and Materials,
Proc. 3rd Int'l Congress (P. Azou, ed.) (1982) p. 491
28. A.R. Troiano, Trans. ASM, 52 (1960), p. 54.
29. R.A. Oriani, Ber. der Bunsen Gesell., 76 (1972), p. 848.
30. G.M. Pressouyre, Metaux Corrosion Industries, No. 666 (1981), p. 11.
31. P. Kedzierzawski, this book.
32. R.A. Oriani, Acta Met., 18 (1970), p. 147.
33. N. Koiwa, Acta Met., 22 (1974), p. 1259.
34. B.A. Novikov et al., Fiz. Metal. Metalloved, 35 (1973), p. 982.
35. H.T. Davis et al., J. Am. Cer. Soc., 58 (1975), p. 446.
36. A.D. Brailsford, J. Nucl. Mat., 60 (1976), p. 257.
37. K. Schroeder, Z. für Physik, 25B (1976), p. 91.
38. D.M. Allen-Booth and J. Hewitt, Acta Met., 22 (1979), p. 171.
39. G.M. Pressouyre and I.M. Bernstein, Corrosion Science, 18 (1978), p. 411.
40. M. Iino, Acta Met., 30 (1982), p. 367 and p. 377.
41. J.B. Leblond and D. Dubois, Acta Met., 31 (1983), p. 1459; and p. 1471.

42. G.M. Pressouyre and I.M. Bernstein, Met. Trans., 9A (1978), p. 1571.
43. G.W. Hong et al., Arch. Eisenhüttenwes., 53 n. 7 (1982), p. 259.
44. K.W. Lange and H.J. Koning, 2nd Int. Conf. on Hydrogen in Metals, 1973, Paris (P. Azou, ed.) paper 1A5.
45. V.I. Saliv et al., Fiz. Metal. Metalloved., 35 (1973), N. 1, p. 119.
46. W. Dresler and M.G. Froberg, JISI (1973), p. 298.
47. I.V. Gavrilin et al., Steel in the USSR, 1973, p. 494.
48. G.S. Ershov and A.A. Kasatkin, Isv. A.N. SSR Metall., (1977) p. 82.
49. H. Kronmüller et al., Phil. Mag., 37B (1978), No. 5, p. 569.
50. M. Weinstein and J.F. Elliott, Trans. AIME, 227 (1963), p. 382.
51. B.T. Lee, J.Y. Lee and S.H. Hwang, Arch. Eisenhüttenwes. 53, No. 2 (1982), p. 71.
52. G.M. Pressouyre, Acta Met., 28 (1980), p. 895.
53. G.M. Pressouyre, Met. Trans., 10A (1979), p. 1571.
54. G.M. Pressouyre, Met. Trans., 14A (1983), p. 2189.
55. R. Gibala and D.S. DeMiglio, Hydrogen Effects in Metal, 1981, (ed. I.M. Bernstein and A.W. Thompson), TMS, Warrendale, PA, p. 113.
56. J.Y. Lee, J.L. Lee and W.Y. Choo, Current Solutions to Hydrogen Problems in Steels, 1982, (C.G. Interrante and G.M. Pressouyre, eds.) ASM, Metals Park, Ohio, p. 423.
57. J. Au and H.K. Birnbaum, Scripta Met., 15 (1981), p. 941.
58. W. Beck et al., Met. Trans., 2 (1971), p. 883.
59. I.M. Bernstein, Scripta Met., 8 (1974), p. 343.
60. T. Kosco and A.W. Thompson, Scripta Met., 16 (1982) p. 1367.
61. J.P. Hirth, Met. Trans., 11A (1980), p. 861.
62. R. Garber, I.M. Bernstein and A.W. Thompson, Met. Trans. A, 12A (1981), p. 225.
63. K. Yoshino and C.J. McMahon, Jr., Met. Trans., 5A, (1974) p. 363.
64. H.Y. Yu and J.C.M. Li, J. Nucl. Met., 20 (1976), p. 872.

65. M. Iino, Met. Trans., 9A (1978), p. 1581.
66. J.C.M. Li, ibid., p. 1353.
67. M. Iino, N. Nomura, H. Takesawa and T. Takeda in Current Solutions to Hydrogen Problems in Steels (C.G. Interante and G.M. Pressouyre, eds.), ASM, Metals Park, Ohio (1982), p. 159.
68. R.M. Latanision, M. Kurkela and F. Lee in Hydrogen Effects in Metal, 1981, (I.M. Bernstein and A.W. Thompson, eds.), TMS, Warrendale, PA, p. 379.
69. M.F. Stevens, Ph.D. Thesis, Carnegie-Mellon University (1984).
70. R. Kerr, F. Guiterrez-Solana, I.M. Bernstein and A.W. Thompson, submitted to Met. Trans.
71. W. Hoffman and W. Rauls, Welding J., 44 (1965), p. 2255.
72. P.G. Bastien, Physical Metallurgy of Stress Corrosion Fracture, (1959), AIME, Interscience, NY.
73. J. Dedieu and L. Pennec, Mem. Sci. Rev. Met., 56 (1959), p. 582.
74. R. Garber, P.J. Grubner and D.L. Sponseller in Hydrogen Effects in Metals (I.M. Bernstein and A.W. Thompson, eds.) (1981), TMS, Warrendale, PA, p. 361.
75. J.P. Frazer and G.G. Eldridge, Corrosion, 14 (1958), p. 524t.
76. A.E. Schuetz and W.D. Robertson, Corrosion, 13 (1957), p. 437t.
77. S. Barnartt, Corr. Sci., 3 (1963), p. 9.
78. E. Snape, Corrosion, 23 (1967), p. 154; 24 (1968), p. 261.
79. C.S. Carter and M.V. Hyatt in Proceedings of International Conference on Stress, Corrosion, Cracking and Hydrogen Embrittlement of Iron Base Alloys, publ. NACE-5, 1973, p. 524.
80. G.M. Waid and R.T. Ault, Corrosion NACE Conf., paper No. 180, 1979.
81. J. Chene, in Current Solutions to Hydrogen Problems in Steels (C.G. Interante and G.M. Pressouyre eds.), (1982) ASM, Metals Park, Ohio p. 263.
82. H. Kihara, Proceedings 7th World Petroleum Conf., Elsevier Press, Disc. 27, 1967.
83. E. Herzog, Ind. Eng. Chem., 53 (1961), 64A.

84. A.P.I. Publ. 941, 2nd Ed., 1977.
85. J.D. Hobson and C. Sykes, J. Iron Steel Inst., 169 (1951), 209.
86. C. Parrini and A. Devito, ASTM-STP, 673 (1979), p. 53.
87. P.J. Grobner et al., Corrosion, 35 (1979), p. 240.
88. C.S. Carter, Corrosion, 25 (1969), p. 240.
89. G.M. Pressouyre, Ph.D. Thesis, Carnegie-Mellon University, (1977).
90. J.A. Marquez, Corrosion, 26 (1970), p. 215.
91. U.P. Levcenko, Cernaja Metallurgija, 10 (1975), p. 116.
92. G.M. Pressouyre and C. Znudzinski, Corrosion NACE Conf., (1982) paper No. 181, 1981.
93. V.M. Tupilko et al., Izv. Vuz. Chern. Met., 4 (1976), p. 131.
94. T. Inoue in Proc. 2nd JIM Int. Symp. on Hydrogen in Metals, Minakami Spa., 1979, p. 433.
95. Current Solutions to Hydrogen Problems in Steels (C.G. Interrante and G.M. Pressouyre eds.) ASM, Metals Park, Ohio (1982). See Chapters on H₂S environments, p. 159ff.
96. A.A. Sheinker, Tech. Rep. ONR, 4 (1978), No. ER.7814-4.
97. I.M. Bernstein, Met. Trans., 1 (1970), p. 3143.
98. A.W. Thompson, Mat. Sci. Eng., 14 (1974), p. 253.
99. G. Sandoz, Met. Trans., 2 (1971), p. 1055; 3 (1972), p. 1169.
100. H.H. Uhlig, Trans. AIME, 158 (1944), p. 183.
101. A.W. Thompson, Materials for Hydrogen Service; "Hydrogen: Its Technology and Implications", Vol. II, ed. K.E. Cox and K.D. Williams, CRC Press, 1977, p. 85.
102. J.W. Thomas and E.W. Klechka, in Effect of Hydrogen on Behavior of Materials (A.W. Thompson and I.M. Bernstein eds.), TMS, Warrendale, PA (1975), p. 542.
103. K.H. Liebchen, Mat. Prot., 4 (1965), p. 50.
104. M. Naguno in Hydrogen Effects in Metals (I.M. Bernstein and A.W. Thompson eds.), TMS, Warrendale, PA (1980), p. 331.
105. J. Beguinot and G.M. Pressouyre, C.L. Tech. Rep., 1980.

No. 80528.

106. T. Kawawa, Trans. ISIJ, 18 (1978), p. 70.
107. G.M. Pressouyre, R. Blandeau and L. Cadiou in Current Solutions to Hydrogen Problems in Steels (C.G. Interrante and G.M. Pressouyre eds.), ASM, Metals Park, Ohio (1982), p. 212.
108. J.P. Fidelle et al., ASTM STP, 543 (1972), p. 221.
109. G.M. Pressouyre, Acta Met., 28 (1980), p. 895.
110. G.M. Pressouyre and I.M. Bernstein, Met. Trans., 12A (1981), p. 835.
111. G.M. Pressouyre and I.M. Bernstein, (Acta Met.), 27 (1979), p. 89.
112. J.A. Brooks and A.W. Thompson in Hydrogen in Metals (I.M. Bernstein and A.W. Thompson eds.), ASM, Metals Park, Ohio (1973), p. 527.
113. M.W. Joosten, T.D. Lee, T. Goldenberg and J.P. Hirth in Hydrogen Effects in Metals (I.M. Bernstein and A.W. Thompson eds.), TMS, Warrendale, PA (1981) p. 839.
114. Y. Yoshino, Corrosion, 38 (1982), p. 156.

TABLE 1 Classification of Traps and Anti-Traps in Ferritic Iron

Type	Traps						Repellers, Obstacles (53, 54)								
	Elements (I) to the left of iron in periodic table						Elements with a negative ϵ_H^I								
Atomic Size	I	E_T	Ref.	I	E_T	Ref.	I	E_T	Ref.	I	E_T	Ref.	I	E_T	Ref.
	Mn	(0.09)	53	Tc	-	-	Ni	(0.08)	53	Mo	-	-	Co		
	Cr	(0.10)	53	Mo	-	-	Mn	(0.09)	53	Zr	0.24	49	Ni		
	V	(0.16)	53	Nb	(0.16)	53	Cr	(0.10)	53	Ti	0.36	42	Cu		
	Ti	0.27	53	Zr	0.24	49	V	(0.16)	53				Zn		
	Ti	0.27	42	Y	1.3	48	Nb	(0.16)	53				Rh		
	Ti	0.5	48				Ce	(0.16)	53				Pd		
	+	0.8	-				O	(0.71)	53				Ag		
	□	-	-				La	(1.0)	53				Ag		
	Sc	-	-				Ta	(1.0)	53				Cd		
							Nd	(1.3)	53						
Linear	Dislocation line: $E_T = 0.2$ to $0.6eV^{(55)}$														
Planar or two dimensional	Interfaces:			E_T			Ref.			Planar defects containing adsorbed repellers (e.g. metalloids)					
	Grain			0.27 to			53								
	Boundaries:			0.80											
	Internal free surfaces:			0.72 to 1.0			55								
Volume	Microvoid:			0.54			56			Volume defects that do not dissolve hydrogen or that induce a compressive matrix stress					
	Void (H_2):			0.30			55								

*Underlined elements: contradictory data exists

E_T is room temperature trapping energy in eV; values in parenthesis are estimated
 is a vacancy with $E_T = 0.5eV^{(55)}$

TABLE II DELETERIOUS SEGREGATING IMPURITIES

IMPURITIES	P	N	Sb	Sn	As	S	Si	Ge	Te	Se	Bi
SEGREGATION PROMOTERS											
MEANS TO AVOID SEGREGATIONS	<ul style="list-style-type: none"> * DECREASE METALLOID CONTENT OF STEEL * REDUCE GRAIN SIZE * INDUCE SEGREGATION OF NOBLE ELEMENTS TO GRAIN BOUNDARIES (E.G. Pt, Pd, ...) * HEAT TREATMENT : E.G. : <ul style="list-style-type: none"> - HEAT ABOVE - 600°C FOR SHORT TIME AND QUENCH. - HOLD BELOW 600°C FOR SOME TIME WHEN COOLING FROM AUSTENITE AND QUENCH - HIGH PRE-HEATING TEMPERATURE PRIOR TO WELDING (TO AVOID STRESS-RELIEF CRACKING) OR RAPID HIGH STRESS RELIEF TREATMENT. * PRODUCE STABLE CARBIDES THAT DO NOT DISSOLVE AND REPRECIPITATE IN THE TEMPERATURE RANGE OF SERVICE. FOR THIS, ONE MAY ADD : <ul style="list-style-type: none"> TITANIUM, TUNGSTEN, MOLYBDENUM, ... * DECREASE THE STEEL CARBON CONTENT * COLD WORK AFTER QUENCHING AND TEMPERING 										

TABLE III

EFFECT OF CHEMICAL COMPOSITION ON HYDROGEN
EMBRIILEMENT SUSCEPTIBILITY

ELEMENT	BENEFICIAL	REF.	DETRIMENTAL	REF.
CARBON	NO EFFECT UP TO 0.5 WTZ	71	PURE IRON	97
	NO EFFECT UP TO 0.2 WTZ	72	LOW STRENGTH IRON	90
	NO EFFECT UP TO 0.5 WTZ	73	Fe-Ni ALLOYS	90
	NO EFFECT FROM 0.15-0.37 WTZ	74	α - STEELS FOR SSC	83
	BENEFICIAL TO SSC*	75	α - STEELS FOR SSC	78
	BENEFICIAL TO SSC AT 0.45Z	4		
NITROGEN	SAME AS CARBON	4	SAME AS CARBON	4
	NO EFFECT UP TO 0.002Z	76	DETRIMENTAL IN γ STEELS (e.g.309)	98
	LINE PIPE STEELS, ABOVE 30 PPM	76	IN γ STEELS	81
MANGANESE	NO EFFECT IN γ STEELS	97	4340, FROM 0.1Z-2.7Z	99
			α STEELS, UP TO 10Z	100
			γ STEELS, UP TO 3Z	4
			α STEELS, FOR SSC	101
			α STEELS, FOR SSC ABOVE 1.5Z	102
			α STEELS, FOR SSC, 0.3Z TO 1.5Z	86
		α STEELS, FOR SSC, UP TO 0.5Z	80	
NICKEL	IN α STEELS ABOVE A CRITICAL AMOUNT	4	IN α STEELS BELOW A CRITICAL AMOUNT	4
	IN γ STEELS; DEPENDS ON CrZ	4	IN α STEELS FOR SSC, ABOVE 1Z	78
	IN α STEELS; NO EFFECT IN SSC	78	IN α STEELS FOR SSC, UP TO 0.8Z	86
	IN α STEELS; NO EFFECT IN SSC	79	IN α STEELS FOR SSC, ABOVE 1Z	80
	IN α STEELS; NO EFFECT UP TO 1Z	80		
	IN γ STEELS; 10-35Z	80		
CHROMIUM	IN α STEELS, AT LOW Z	4	IN α STEELS	75
	IN γ STEELS, DEPENDS ON NiZ	4	IN α STEELS FOR SSC UP TO 5Z	79
	IN α STEELS VS SSC, UP TO 1.4Z	82	IN α STEELS, AT 2.4Z	103
	IN α STEELS, BETWEEN 2-2.5Z	83		
	FOR HYDROGEN ATTACK	84		
	IN α STEELS AT 3.3Z	85		
	IN α STEELS FOR SSC, UP TO 1Z	86		
IN α STEELS FOR SSC, UP TO 2Z	80			
MOLYBDENUM	IN α STEELS FOR SSC	83	IN Fe-Ni ALLOYS	90
	IN α STEELS FOR SSC, UP TO 0.7Z	80	IN α STEELS FOR SSC	75
	NO EFFECT ON SSC IN α STEEL, 0.5Z MAX	86	IN α STEELS FOR SSC, ABOVE 0.7Z	80
	IN α STEELS FOR SSC, 0.75-0.90Z	87	IN γ STEELS BELOW 1.5Z	4
	IN γ STEELS ABOVE 1.5Z	4		
	IN α STEELS, VS HYDROGEN ATTACK	84		
SILICON	IN 4340 STEEL, UP TO 2Z	88	IN α STEELS, 0.25Z-2Z	80
	IN α HIGH STRENGTH STEELS	4		
	IN γ STEELS, PARTICULARLY ABOVE 4Z	4		
	IN α STEELS FOR SSC, 0.3-0.9Z	86		
TITANIUM	IN IRON, INTERNAL HE, UP TO 1.5Z	89	MARAGINGS, IF Ni, Ti PRESENT	76
	IN α STEELS	78	IN γ STEELS, SMALL ADDITIONS	4
	IN α STEELS	90	IN α STEELS FOR SSC, 0.17-0.35Z	80
	IN α STEELS	4	IN α STEELS FOR SSC, AT 0.09Z	78
	IN γ STEELS	4		
	PROBABLY FOR HYDROGEN ATTACK	-		
IN α STEEL FOR FLAKING	91			
VANADIUM	IN α STEELS FOR SSC	83		
	IN α STEELS FOR SSC	92		
	IN α STEELS FOR SSC UP TO 0.2Z	80		
	IN α STEELS FOR SSC	86		
	IN γ STEELS	4		
NIOBIUM	IN α STEELS FOR SSC	80		
	NO EFFECT, SSC, UP TO 0.1	86		
	IN α STEEL, AT 0.44Z	93		
ZIRCONIUM	AS FOR TITANIUM	79	AS FOR TITANIUM	79
	IN α STEEL FOR FLAKING	91		
	IN α STEEL, AT 0.047Z	93		
ALUMINIUM	IN α STEELS FOR SSC, 0.3-0.6Z	82	VARIABLE IN γ STEELS	4
	IN γ STEELS	4		
	IN α STEELS FOR SSC	80		
	IN α STEELS FOR SSC, UP TO 0.5Z	86		
BORON	IN α STEELS UP TO $4 \times 10^{-3}Z$	94		
COBALT	IN γ STEELS	4		
	LINE PIPE STEELS FOR SSC	63		
	NO EFFECT FOR SSC	80		
COPPER	NO EFFECT OR BENEFICIAL, SSC,	95	α STEELS FOR SSC, UP TO 0.5Z	86
	α STEELS	80		
	NO EFFECT ON α STEELS: SSC			
TUNGSTEN	NO EFFECT, SSC α STEELS, UP TO 0.75Z	80		
RARE EARTH (La, Ta, Ce)	NO EFFECT, SSC α STEELS, UP TO 0.5Z	80		
	α STEELS FOR FLAKING	96		
PALLADIUM	α STEELS FOR SSC	95		
	4340 VS FLAKING, UP TO 0.3Z	91		

*SSC: SULFIDE STRESS CRACKING

TABLE IV

EXAMPLES OF TRAP ADDITIONS TO STEELS

ADDITION	TYPE OF TRAP	QUANTITY	EFFECT	REFERENCE
PALLADIUM	PROBABLY ATOMIC REPELLER	0.30%	ADDED TO 4340 STEEL, LEADS TO DISAPPEARANCE OF FLAKING	91
TITANIUM	ATOMIC TRAP	0.09%-1.5%	REDUCES BY A FACTOR OF THREE HIC OF PURE IRON, MAY NOT BE A GOOD ADDITION IN CASE OF INTERNAL HYDROGEN EMBRITTLEMENT	110,111
CERIUM LANTHANUM	ATOMIC TRAP	0.02%-0.2%	REDUCES FLAKING SENSITIVITY IF UNIFORM DISTRIBUTION; NO EFFECT IF HETEROGENEOUS DISTRIBUTION	96
TITANIUM	CARBIDES	0.14%-0.37%	REDUCES FLAKING OF 4340 STEEL	91
ZIRCONIUM	CARBIDES	0.3% 0.047%	REDUCES FLAKING OF 4340 STEEL HELPS KEEP DUCTILITY AFTER ELECTROCHEMICAL TREATMENT	91 93
NIObIUM	CARBIDES	0.44%	HELPS KEEP DUCTILITY AFTER ELECTROCHEMICAL TREATMENT	93
BORON	NITRIDES	0.0001% 0.0039% N: .002- .006%	BENEFICIAL ADDITION AS LONG AS BN IS NOT DISTRIBUTED ON BOUNDARIES	94
THORIUM	OXIDES	2%	ADDED TO NICKEL, FAVOURABLE AFTER WELDING IF OXIDES ARE NOT DISSOLVED OR IN INTERNAL HYDROGEN EMBRITTLEMENT	112,113
TITANIUM NIObIUM VANADIUM MOLYBDENUM	FINE COHERENT CARBIDES	C: 0.18-0.41% V: → 0.1% Mo: .27-.92% Ti: → 0.5% Nb: → 0.5%	ADDED TO LOW ALLOY STEELS, APPEARS BENEFICIAL, OR AT LEAST NOT DETRIMENTAL, TO SULFIDE STRESS CRACKING RESISTANCE	114
PALLADIUM COBALT TITANIUM CALCIUM	} ATOMIC -----> NITRIDES	1% 0.2% - -	ADDED TO LINEPIPES STEELS; LED TO VARIOUS IMPROVEMENTS OF BEHAVIOUR IN SOUR ENVIRONMENTS	65

Table V

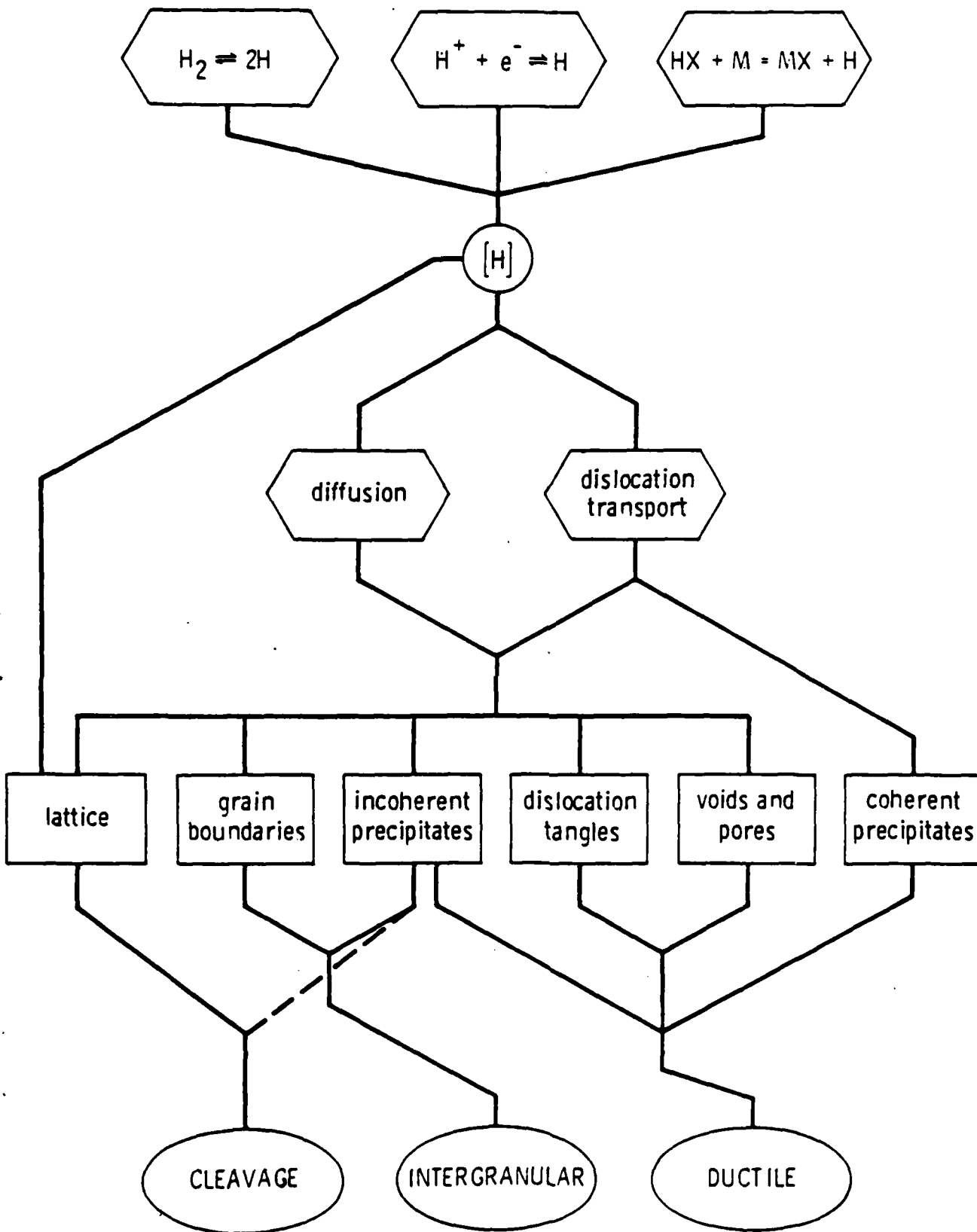
Heat Treatment and Subsequent Microstructure of HY130 and 300M

C Mn Ni Cr Mo V Si

HY130 .09 .754.99.61.54.07 -

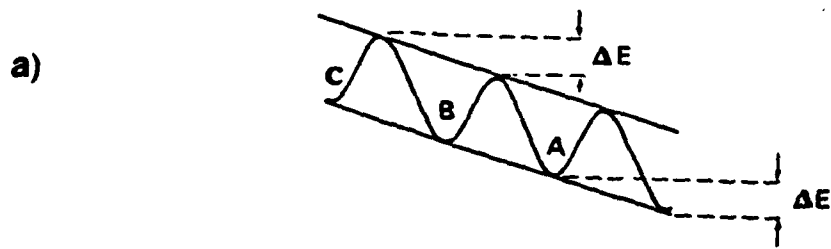
300M .41 .731.83.74.38.07 1.5

HY130		300M	
HEAT TREATMENT	MICROSTRUCTURE	HEAT TREATMENT	MICROSTRUCTURE
Austenitize 1 hr. at 900C, oil quench (OO)	Autotempered martensite	Austenitize 1 hr. at 900C, oil quench, temper 2 hrs. at 450C (OOA1T)	Tempered martensite, retained austenite(5%)
Austenitize 1 hr. at 900C, air cool (AC)	Martensite, lower bainite, retained austenite(5%)	Austenitize 1 hr. at 900C, oil quench, anneal 1 hr. at 780C, isothermally transform 3 hrs. at 350C (QAAT7)	Lath ferrite, martensite, lower bainite, retained austenite(20%)
Austenitize 1 hr. at 900C, oil quench, anneal 1 hr. at 675C, isothermally transform 3 hrs. at 375C (QAAT7)	Lath ferrite, martensite, retained austenite(5%)	Austenitize 1 hr. at 900C, oil quench, anneal 1 hr. at 780C, oil quench (QAQO0)	Lath ferrite, martensite, retained austenite(10%)
Austenitize 1 hr. at 900C, oil quench, anneal 1 hr. at 675C, oil quench (QAQO0)	Lath ferrite, martensite, retained austenite(10%)	Austenitize 1 hr. at 900C, oil quench, temper 2 hrs. at 650C (OOA1T)	Tempered martensite
Austenitize 1 hr. at 900C, isothermally transform 18 hrs. at 395C (IT)	Martensite, lower bainite, retained austenite(5%)	Austenitize 1 hr. at 900C, oil quench, anneal 1 hr. at 745C, oil quench (QAQO0)	Lath ferrite, martensite
Austenitize 1 hr. at 900C, oil quench (QAQO0)	Lath ferrite, martensite, retained austenite(5%)	Austenitize 1 hr. at 900C, oil quench, anneal 1 hr. at 745C, oil quench, immerse 1 hr. at -196C (QAQO0)	Lath ferrite, martensite
Austenitize 1 hr. at 900C, oil quench, anneal 1 hr. at 720C, oil quench, immerse 1 hr. at -196C (QAQO0)	Lath ferrite, martensite	Austenitize 1 hr. at 900C, oil quench, anneal 1 hr. at 700C, oil quench (QAQO0)	Lath ferrite, lower bainite, martensite
Austenitize 1 hr. at 900C, oil quench, anneal 1 hr. at 700C, oil quench (QAQO0)	Lath ferrite, lower bainite, retained austenite(5%)		
Austenitize 1 hr. at 900C, oil quench, anneal 1 hr. at 700C, leathermally transform 3 hrs. at 375C (QAAT7)	Lath ferrite, lower bainite, martensite		

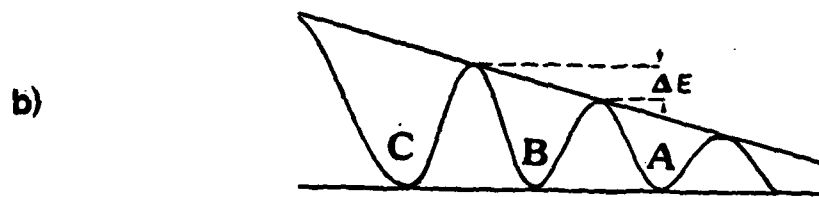


Summary of hydrogen processes (hydrogen sources, hydrogen transport) and microstructural locations, with corresponding end results (hydrogen in solution, fracture). See the text for discussion and examples. Dashed line at the bottom refers to cleavage of hydrides.

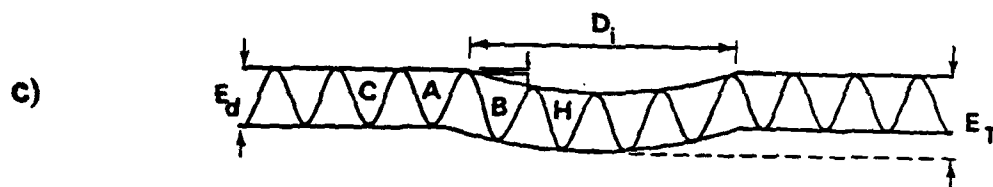
FIG. 1



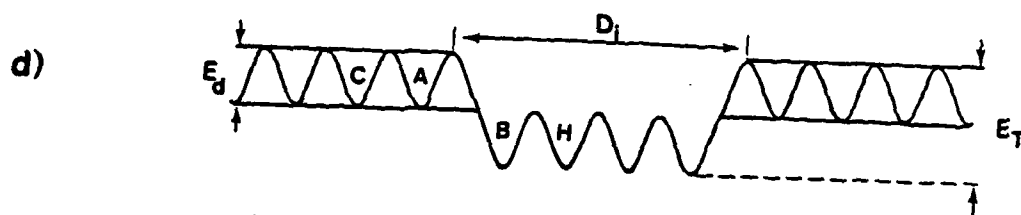
a) role of attractive forces on hydrogen diffusion



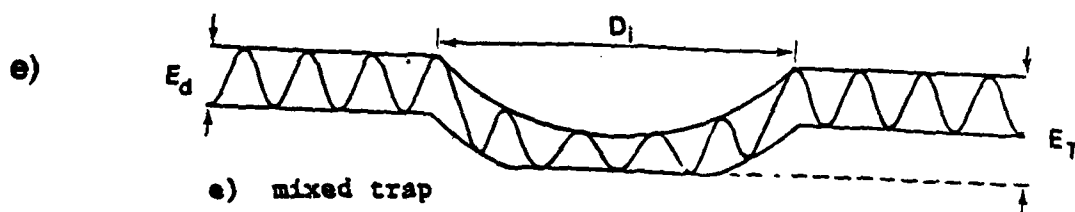
b) role of physical perturbation on hydrogen diffusion



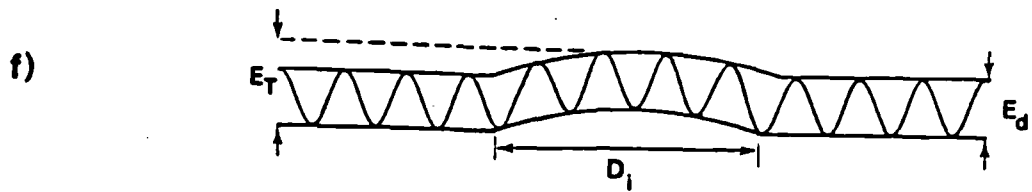
c) attractive trap



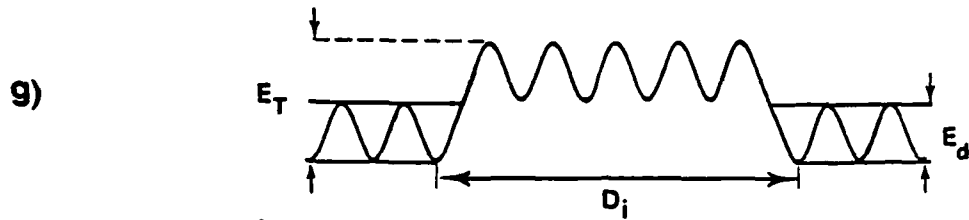
d) physical trap



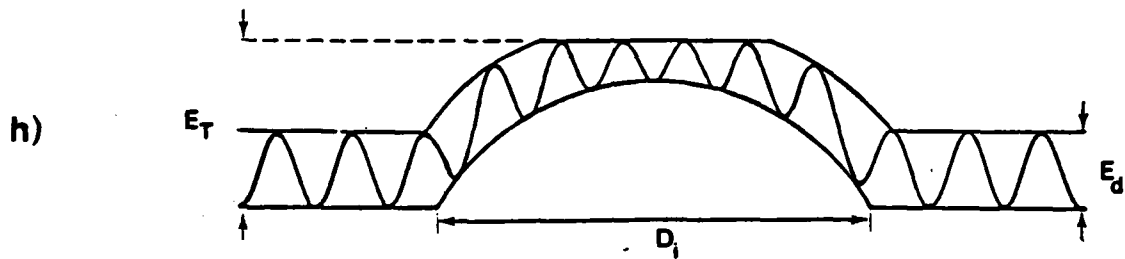
e) mixed trap



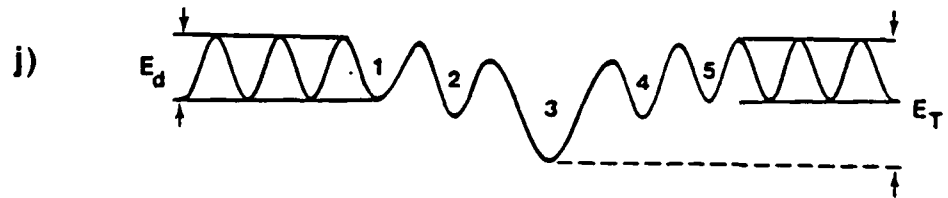
f) repeller



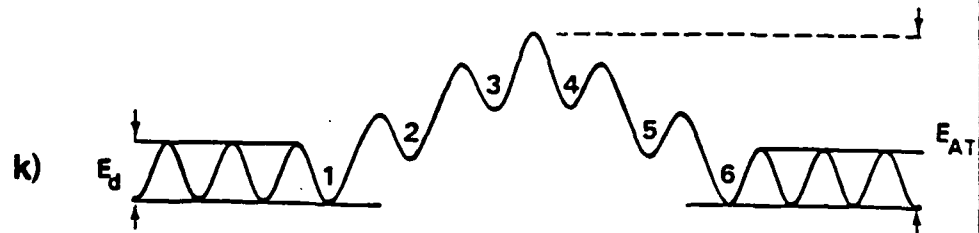
g) obstacle



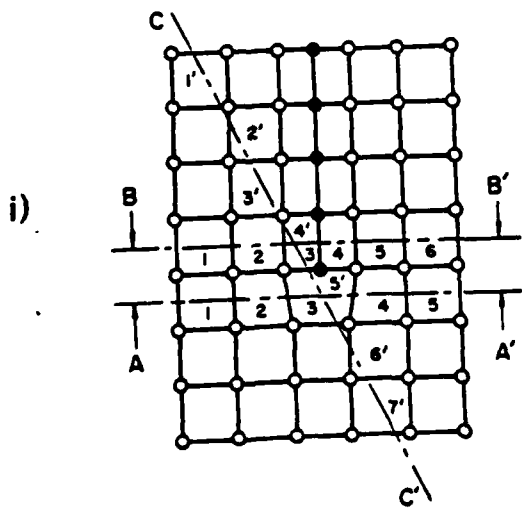
h) mixed anti-trap



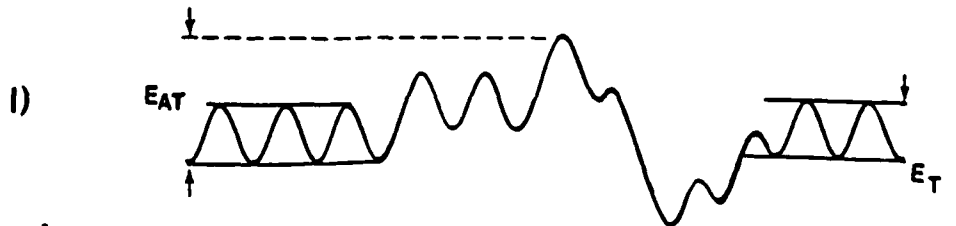
j) schematic for hydrogen diffusion along A-A'
(attractive trap region)



k) schematic for hydrogen diffusion along B-B' (repeller region)



i) edge dislocation on an interaction center for hydrogen



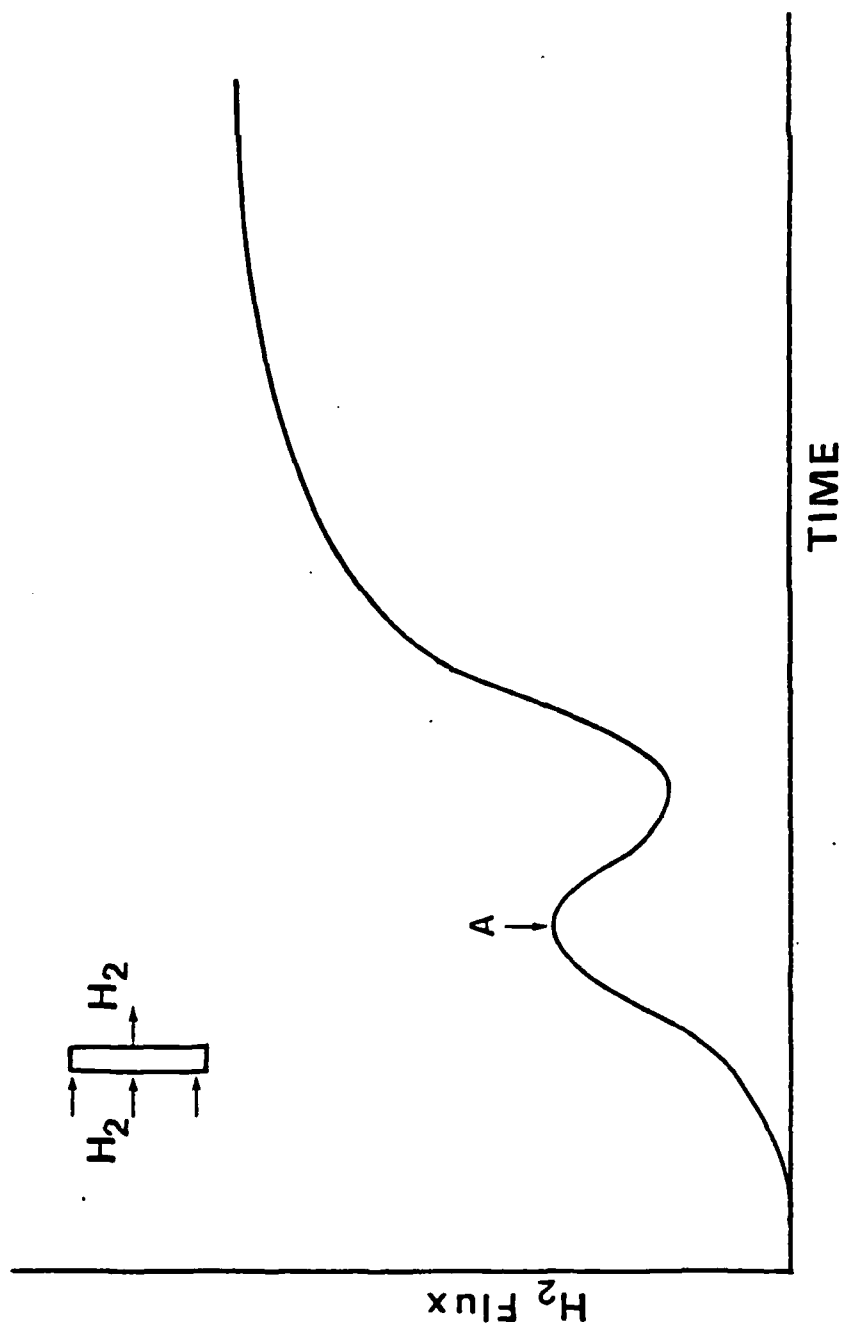
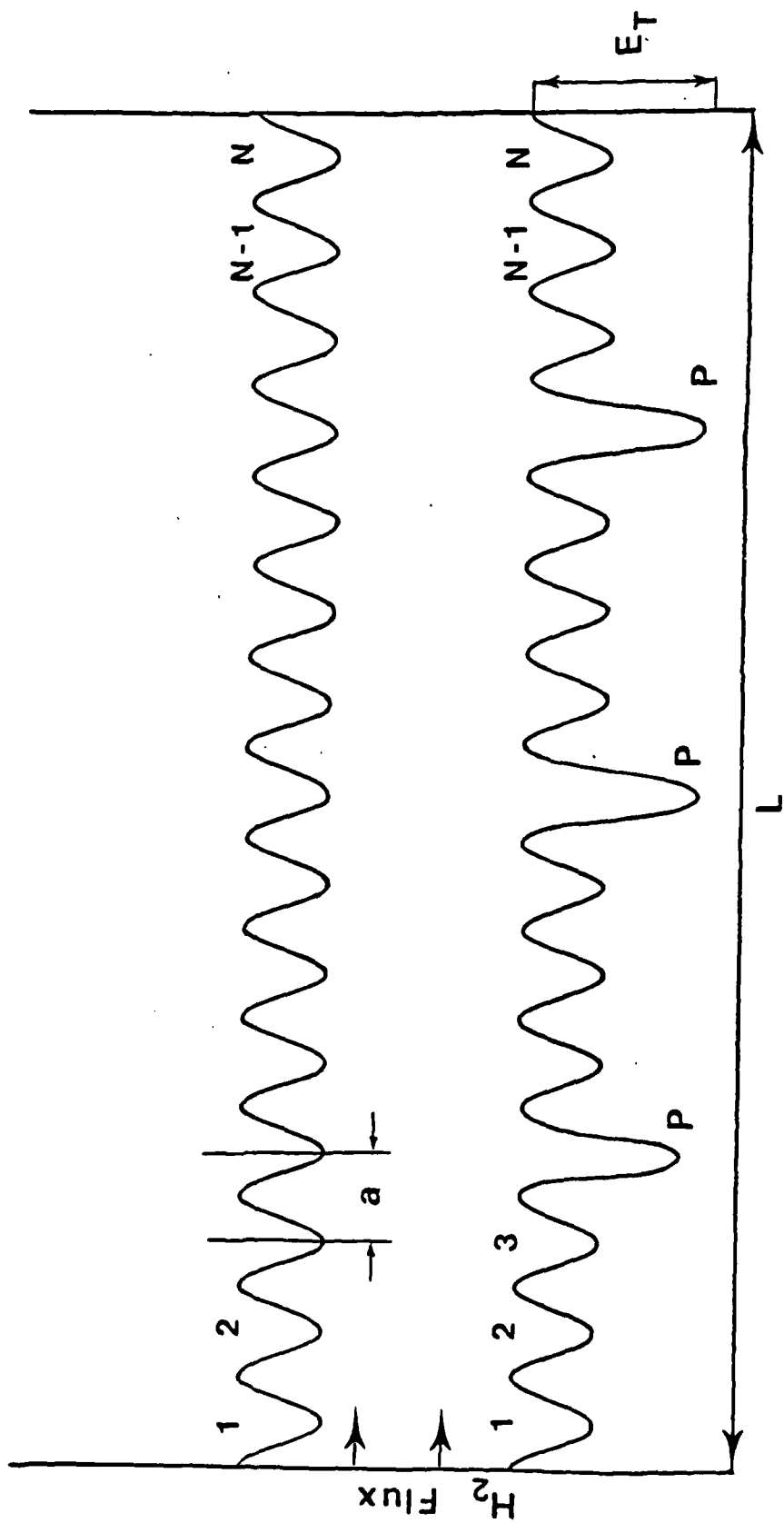


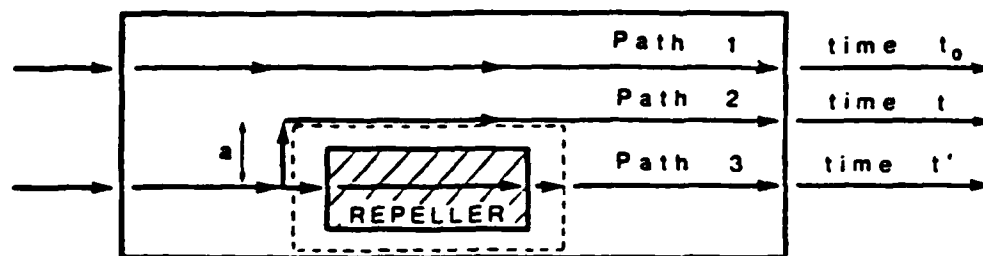
FIG. 3

Evidence for the evaluation of traps in a δ -Mn steel cathodically charged in INH_2SO_4 at a current density of $10^{mA/cm^2}$. Cracks were found in point A associated with a decrease in hydrogen permeability.



Effect of traps on the effective (apparent) diffusivity of hydrogen. Compare the schematic of the perfect lattice (4a) with that containing N_p trapping sites (4d).

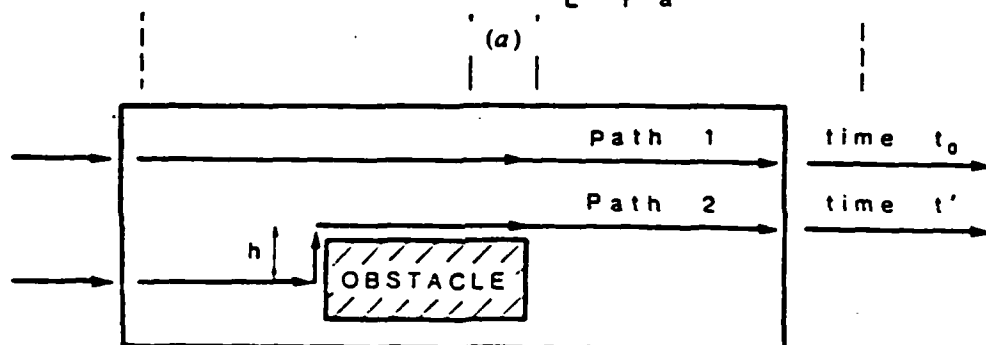
FIG. 4



• Simple diffusion : $t_0 \simeq L^2 / D_0$

• With repeller : $t \simeq t_0 + a^2 / D_0 = L^2 / D_a$

and $D_a \simeq \left(\frac{L^2}{L^2 + a^2} \right) \cdot D_0 < D_0$



• Simple diffusion : $t_0 \simeq L^2 / D_0$

• With obstacle : $D'_a \simeq \left(\frac{L^2}{L^2 + h^2} \right) \cdot D_0$

$D_0 < D'_a < D_0$

(b)

Schematic of diffusion with repellers and obstacles. (a) t_0 : time to diffuse through "L", without repeller, path '1'. D_0 : diffusion coefficient in perfect lattice. t : time to diffuse when hydrogen goes around the repeller, path '2'. t' : time to diffuse when hydrogen goes over the repeller (or inside its interaction zone), path '3'. a : width of the zone where the repulsive force is exerted. D_a : apparent diffusion coefficient with repeller. (b) Same as (a), with obstacle. h : width of obstacle.

FIG. 5

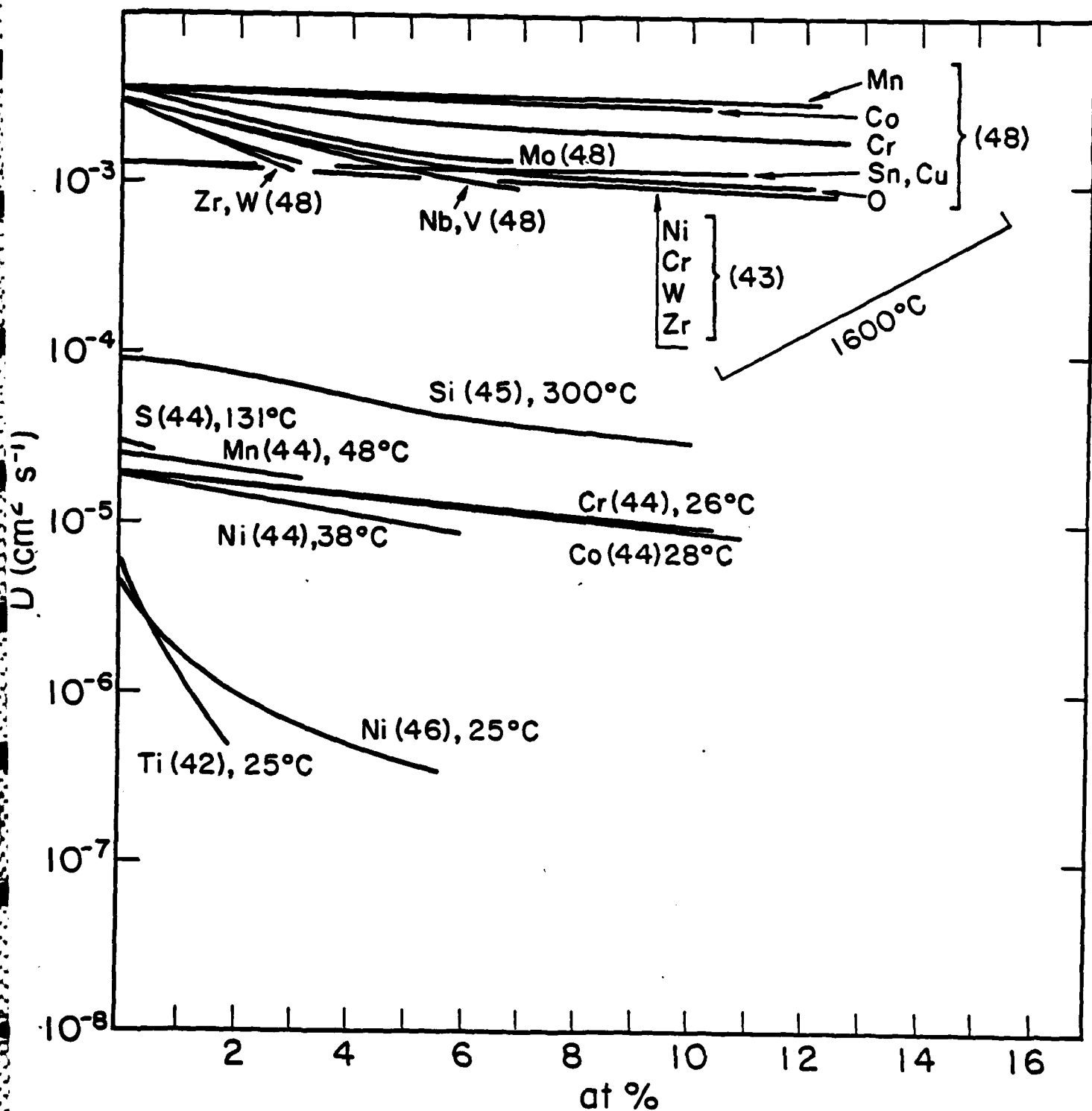
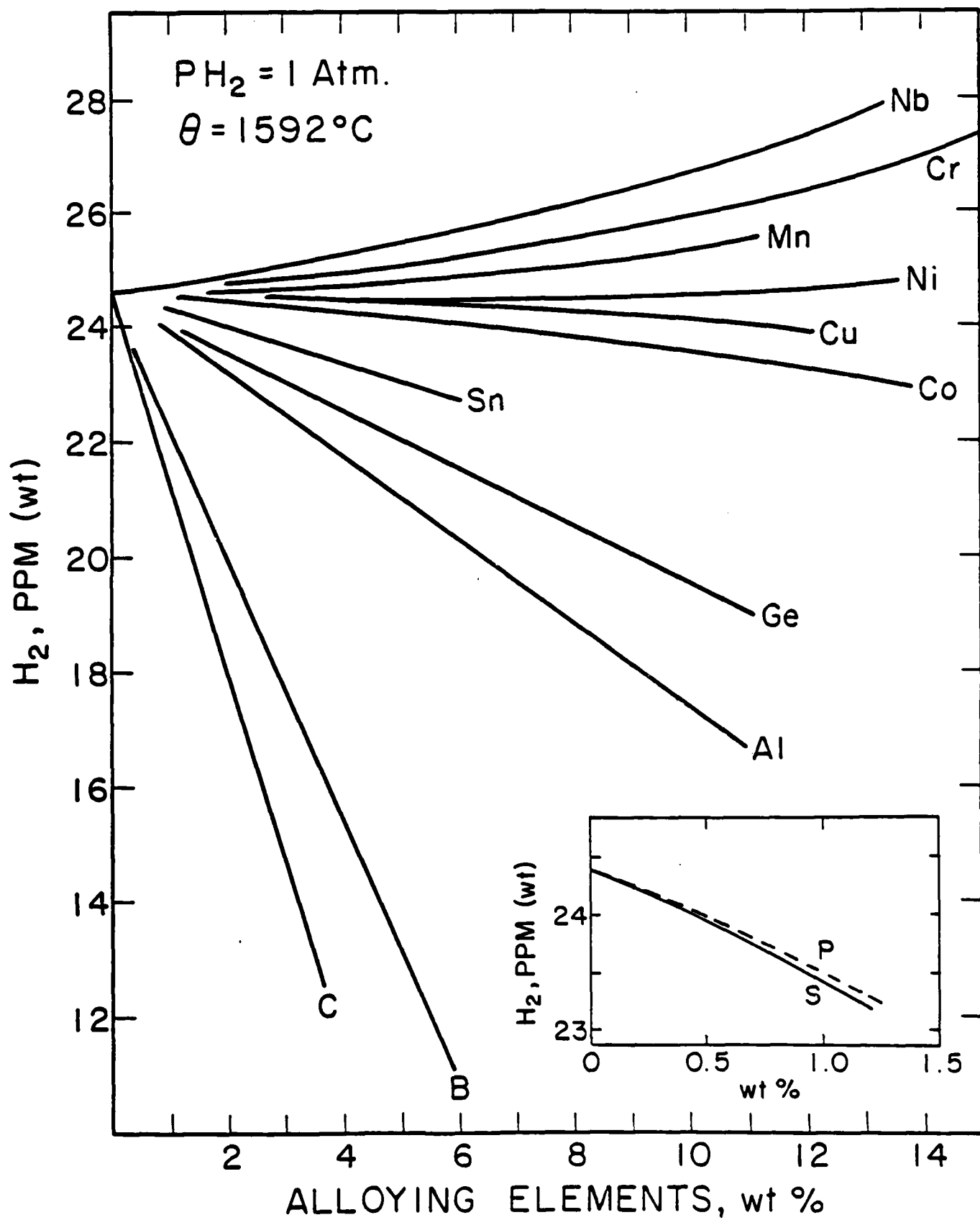


FIG.6

Effect of alloying elements in iron on hydrogen diffusivity at different temperatures. Numbers in parentheses are source references.



a) Solubility of hydrogen in liquid iron containing different alloy contents.⁵⁰

FIG. 7a

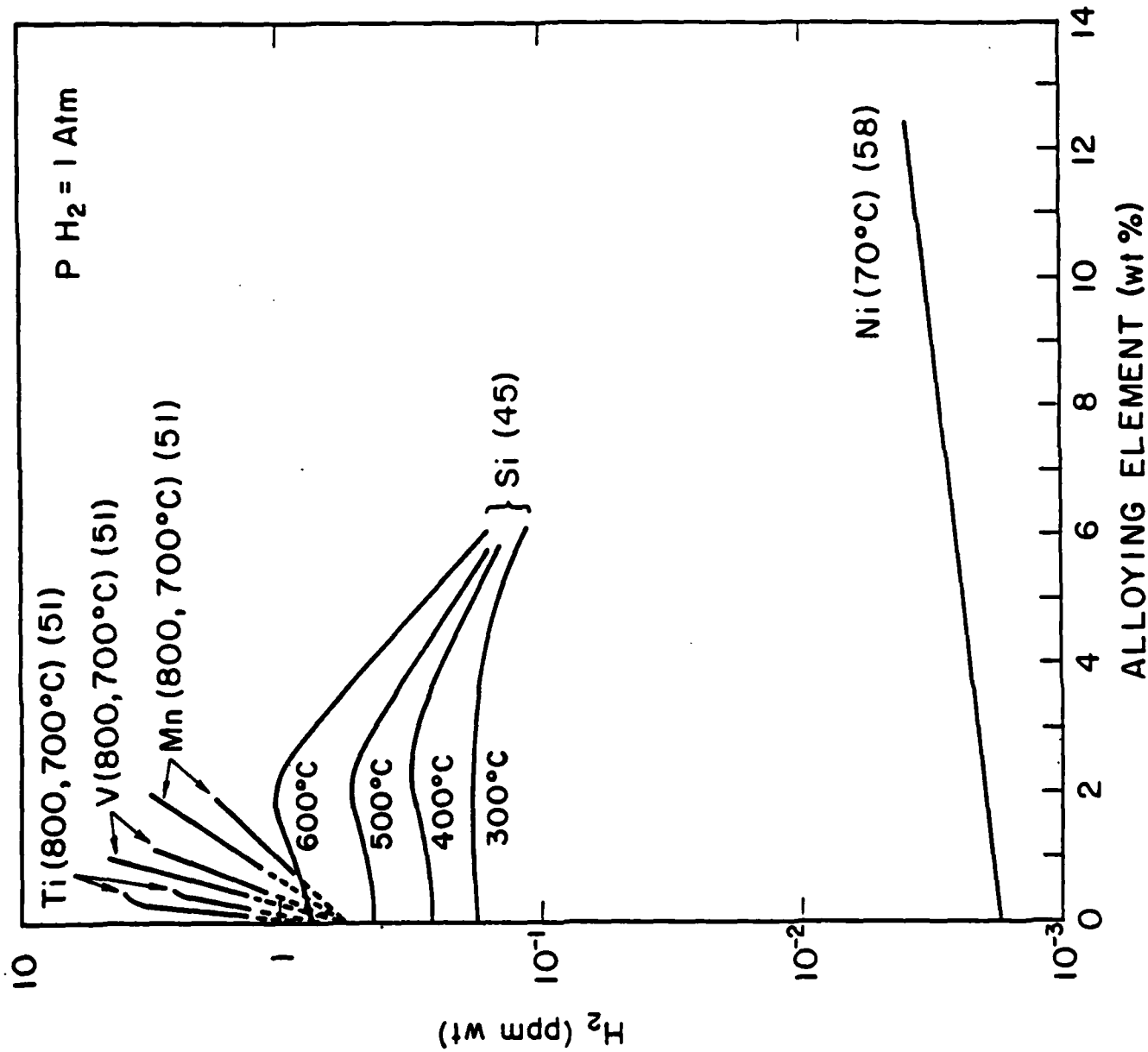


FIG. 7b b) Solubility of hydrogen in solid iron for different temperatures and different alloy contents. Source references are in parentheses.

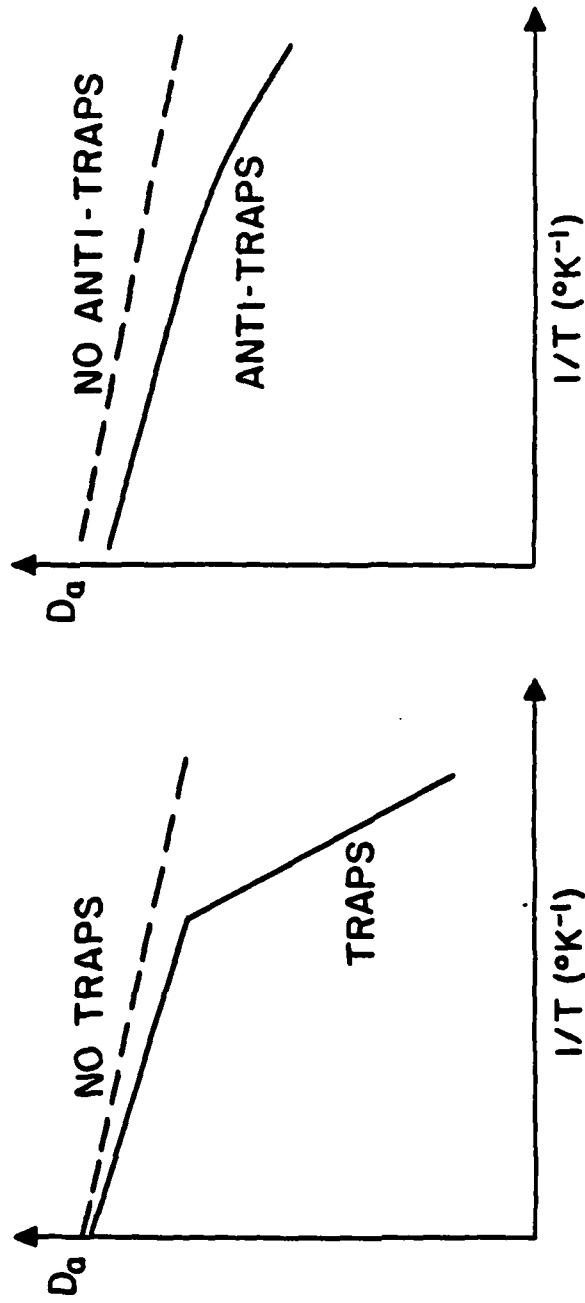


FIG. 8

Schematic of effect of traps and anti-traps on the temperature dependence of the effective hydrogen diffusivity.

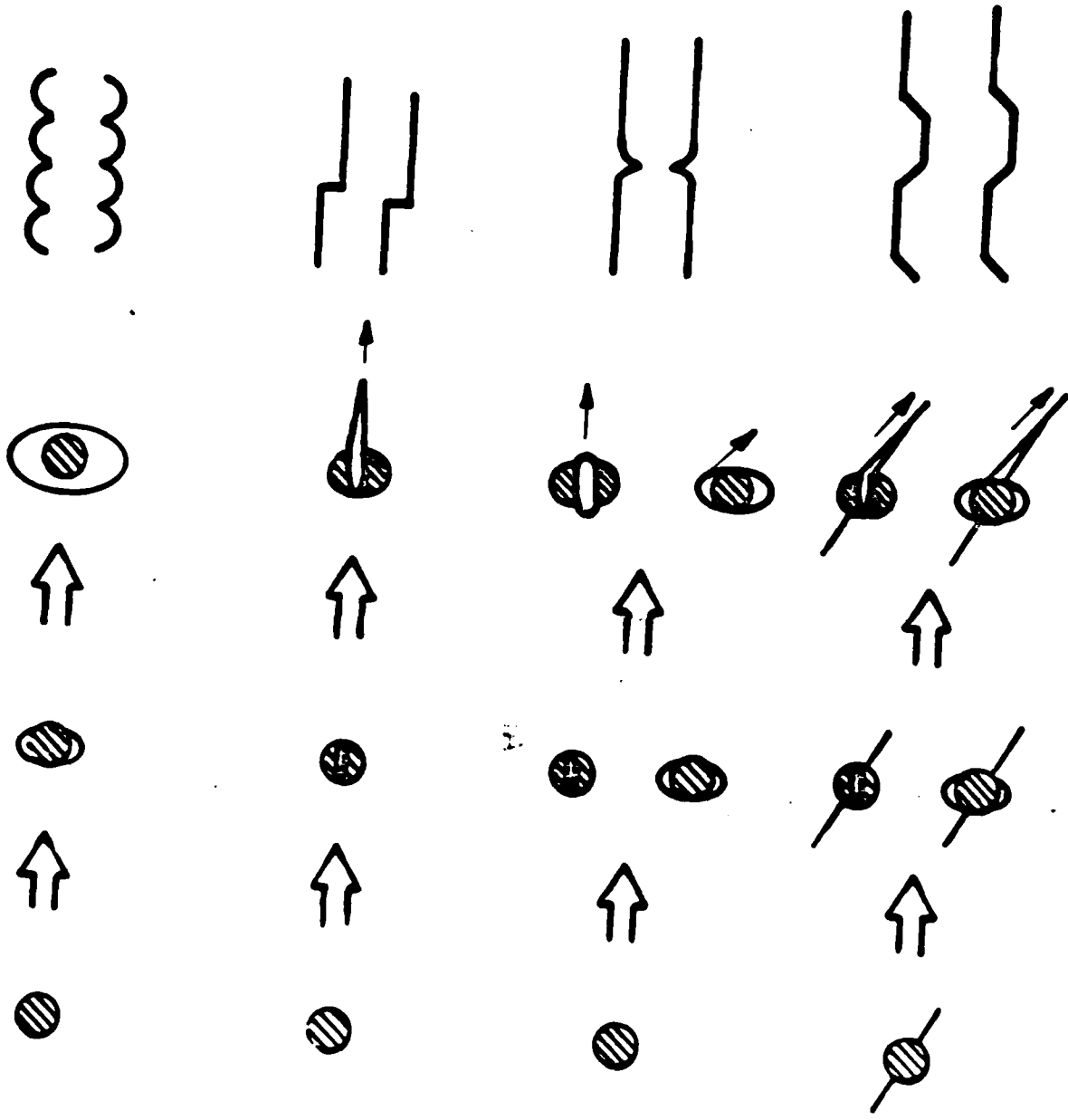


FIG. 9 The possible role of particles in nucleating in turn microvoid
 coalescence; cleavage; quasi-cleavage; intergranular or

Parameters which can affect the critical concentration (C_k) for hydrogen induced crack initiation and the amount of hydrogen trapped at a particular defect.⁵

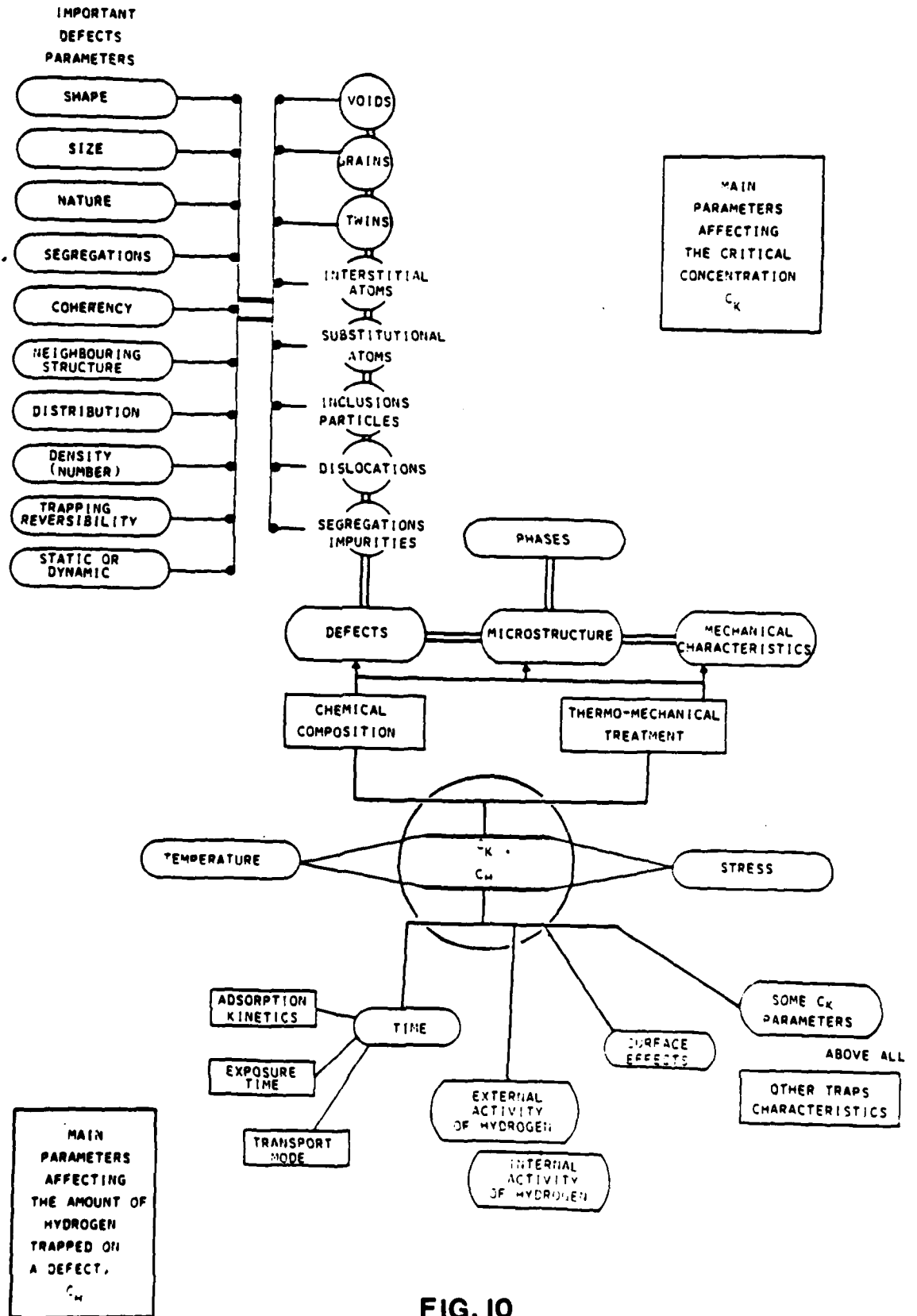


FIG. 10

Hydrogen pressure developed in voids of different shape factor (different c/a ratios).⁵⁴

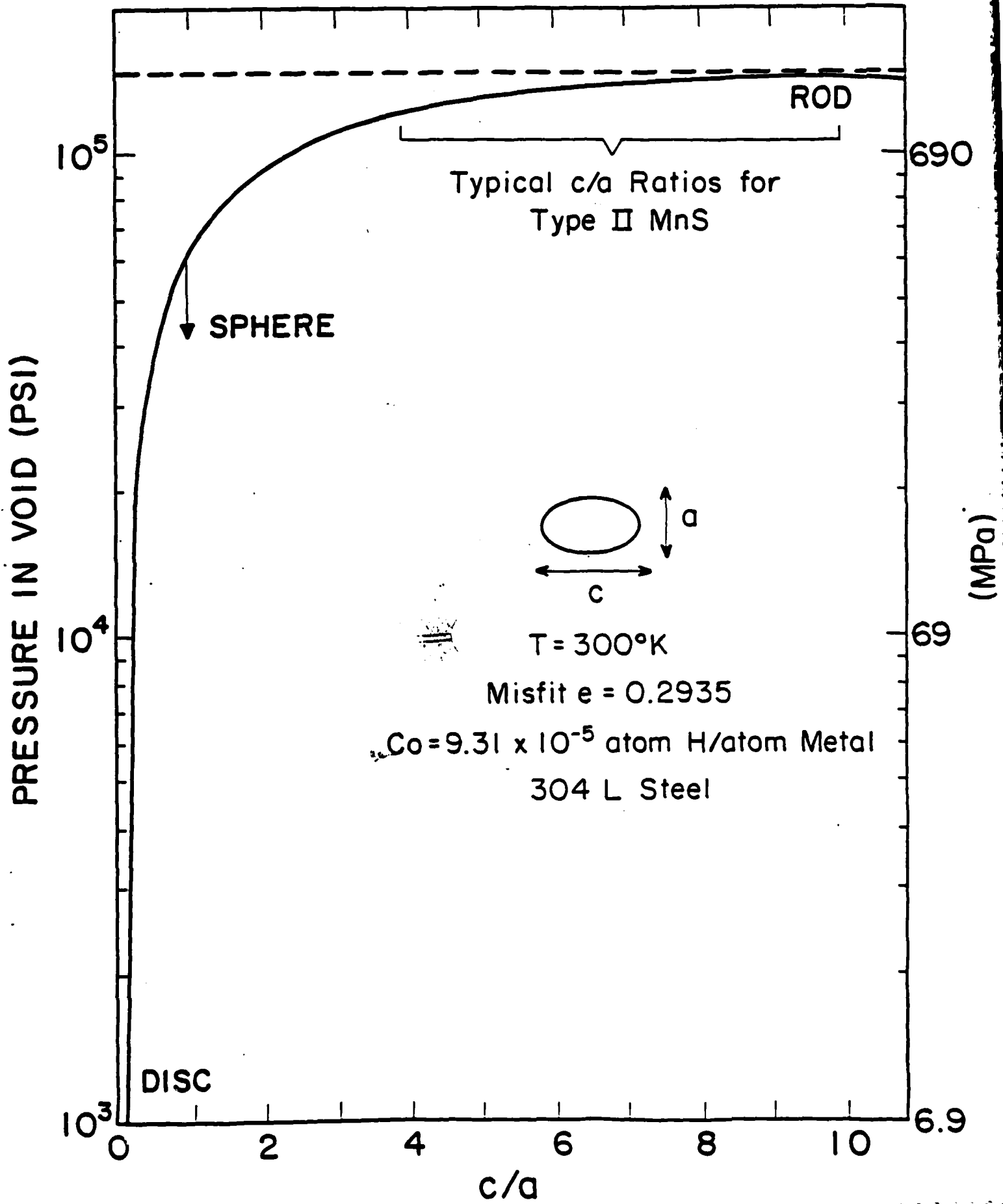
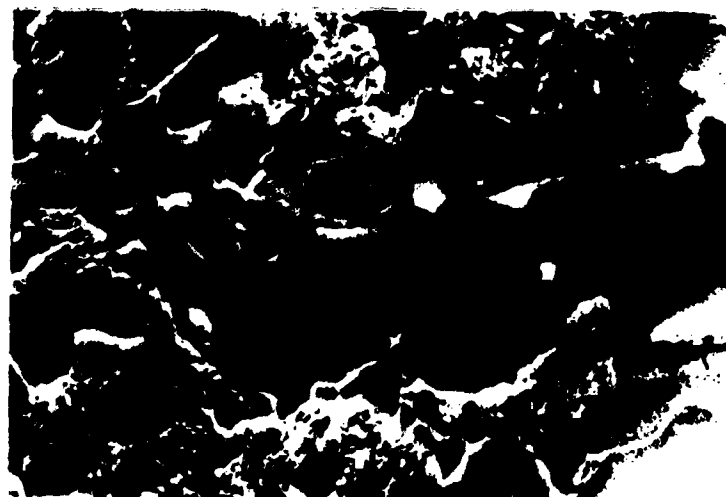
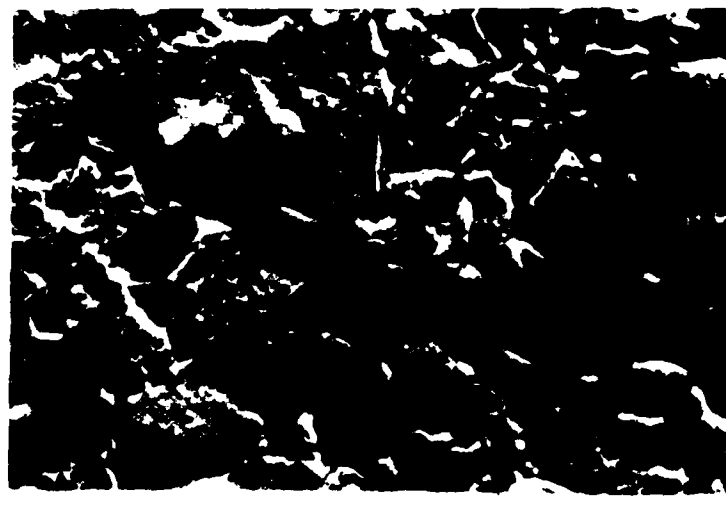


FIG. 11 Hydrogen



Examples of cathodically induced hydrogen cracks initiated at the sharp extremities of a MnS inclusion.

FIG. 12

EXAMPLE OF TYPICAL CA-RE TREATMENTS
FOR INCLUSION SHAPE CONTROL

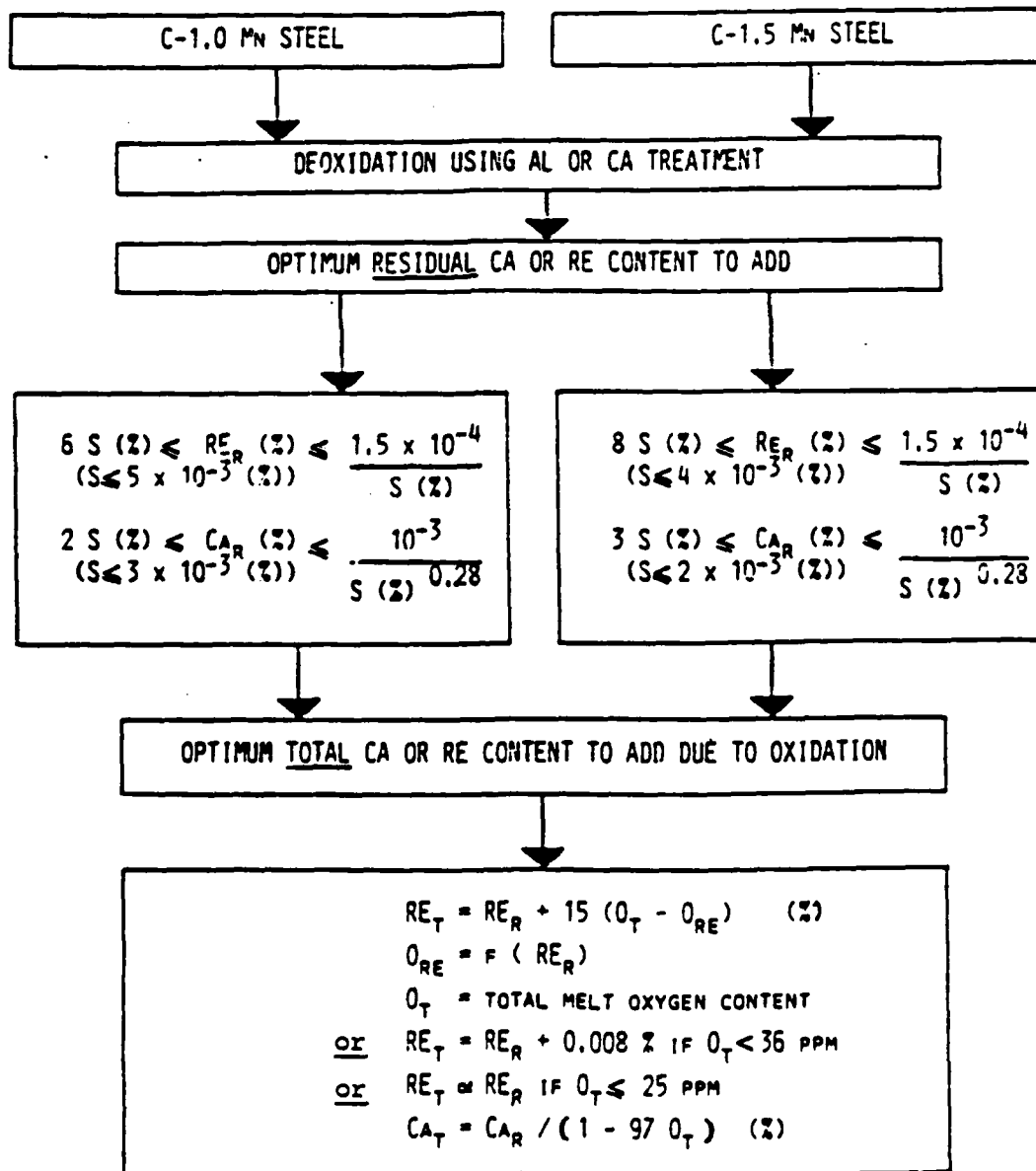
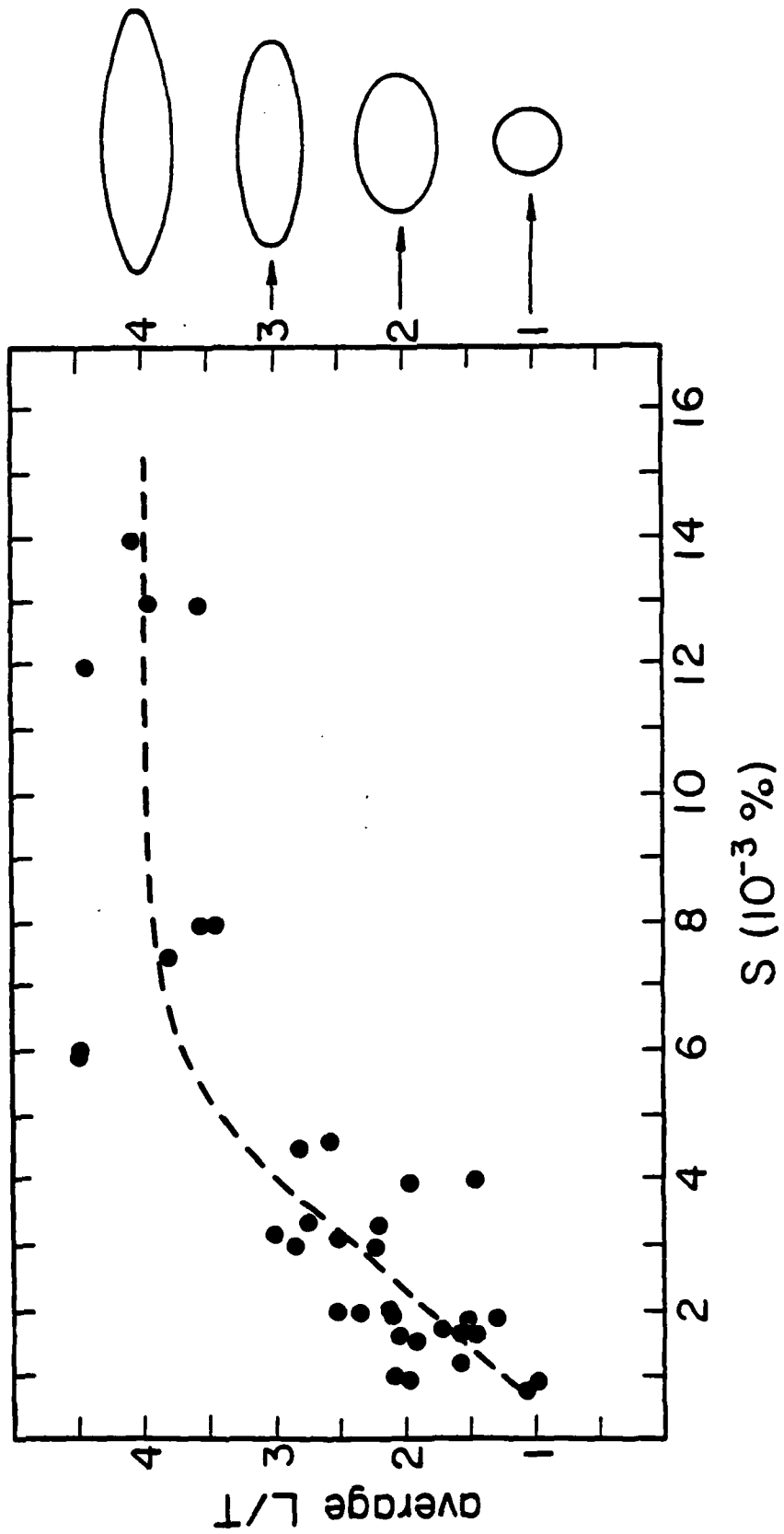


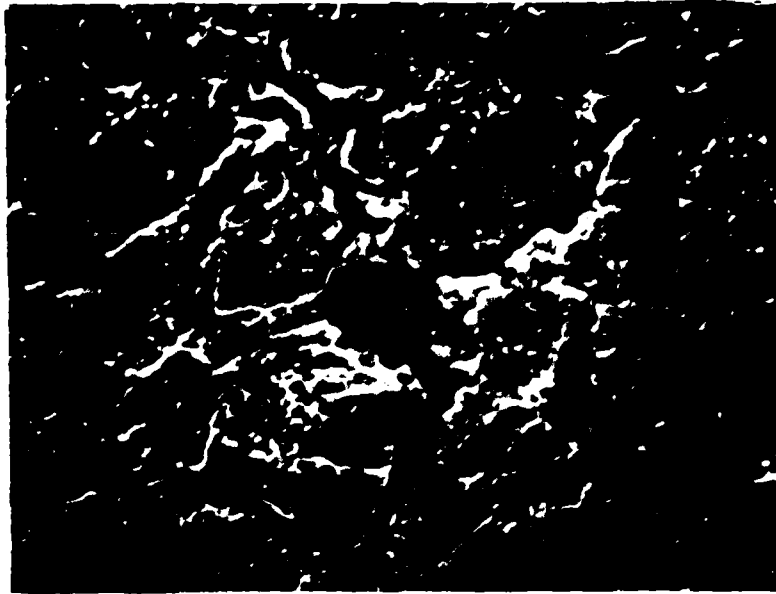
FIG.13

Some typical calcium-rare earth treatments for inclusion shape control RE_T , CA_T and RE_R . CA_R are the total and residual rare earth and calcium contents respectively. The empirical relations to determine RE_T are



Effect of sulfur content on the shape of MnS particles in a normalized C-Mn steel. (5)

FIG.14



Cathodically-induced hydrogen cracking from a large round oxisulfide in
a 3.5 Ni steel.

FIG. 15

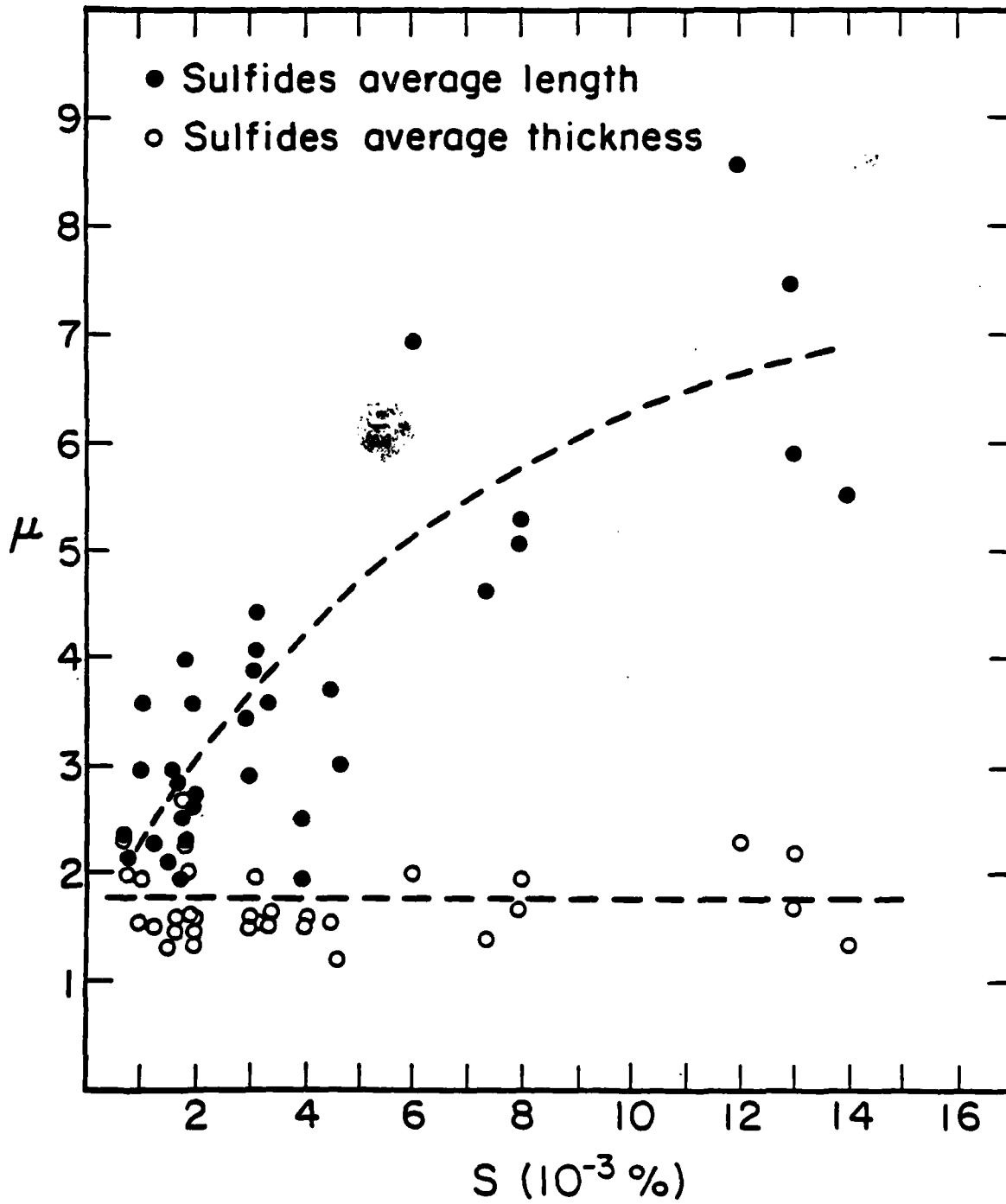
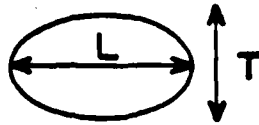


FIG. 16

Effect of sulfur content of average length and thickness of sulfides (in microns, μ).

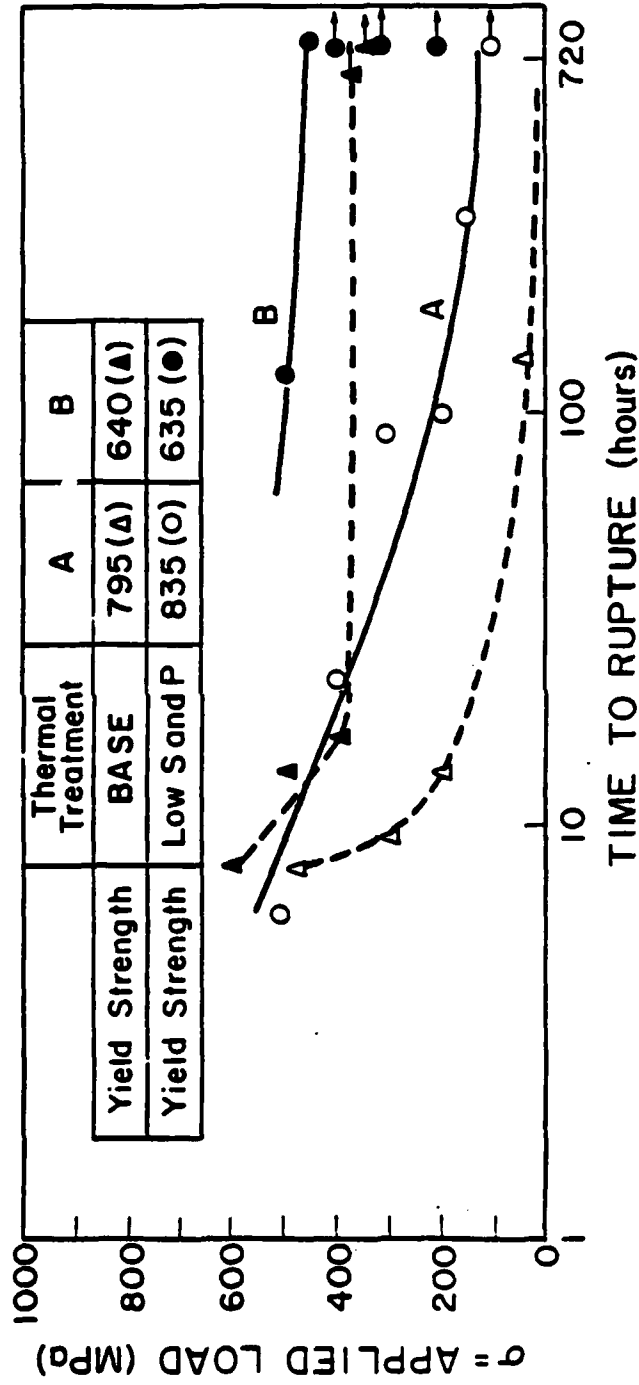


FIG.17

Delayed ruptured testing in H_2S NACE solution for two 4140 type steels, treated to have "normal" sulfur and phosphorous contents of $21 \times 10^{-3}\%$ and $21 \times 10^{-3}\%$ respectively and "low" contents of $5 \times 10^{-3}\%$ and $6 \times 10^{-3}\%$ respectively.

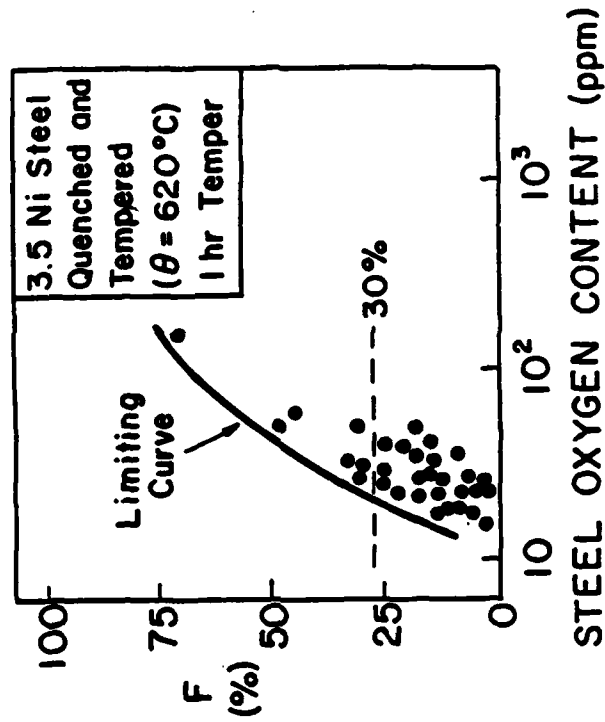
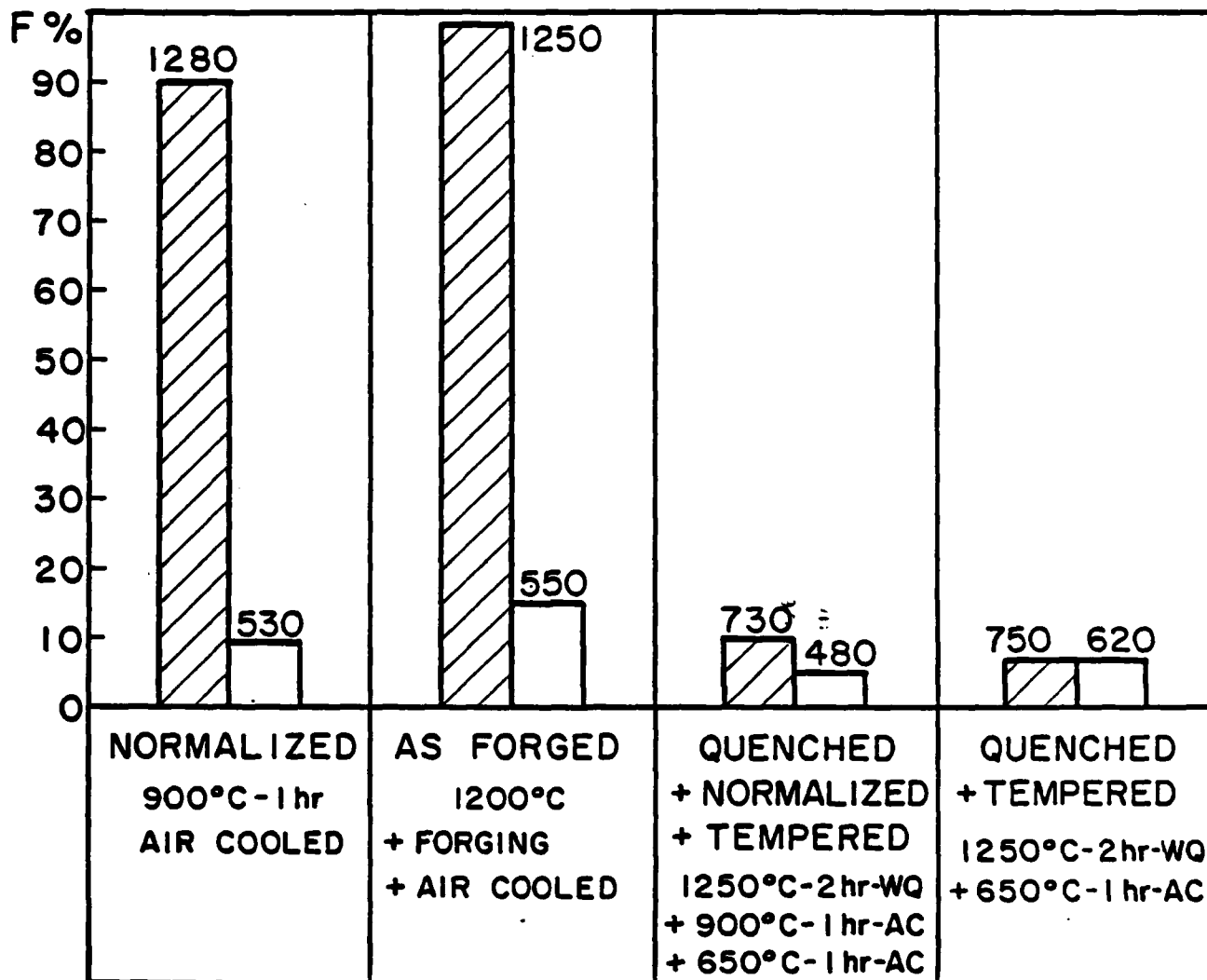




FIG. 18

Effect of steel oxygen content on the hydrogen embrittlement susceptibility of a 3.5 Ni steel. (5) The index F is the reduction in area loss due to hydrogen defined by $F\% = \frac{\%RA_{II}}{\%RA_{I}} \times 100$ where $\%RA_{II}$ and $\%RA_{I}$ are the

reduction of area at fracture with and without hydrogen. The lower is F the more resistant the steel.



 C-Mn steel with "segregated zone" composition
(C-0.27, Mn-2.3, Si-0.6, S-0.013, P-0.020 wt %)

 C-Mn steel with "clean zone" composition
(C-0.17, Mn-1.3, Si-0.3, S-0.004, P-0.004 wt %)

Numbers close to bar, are σ_{UTS} in MPa

FIG.19

Effect of heat treatment and chemical composition on hydrogen embrittlement susceptibility as measured by F.

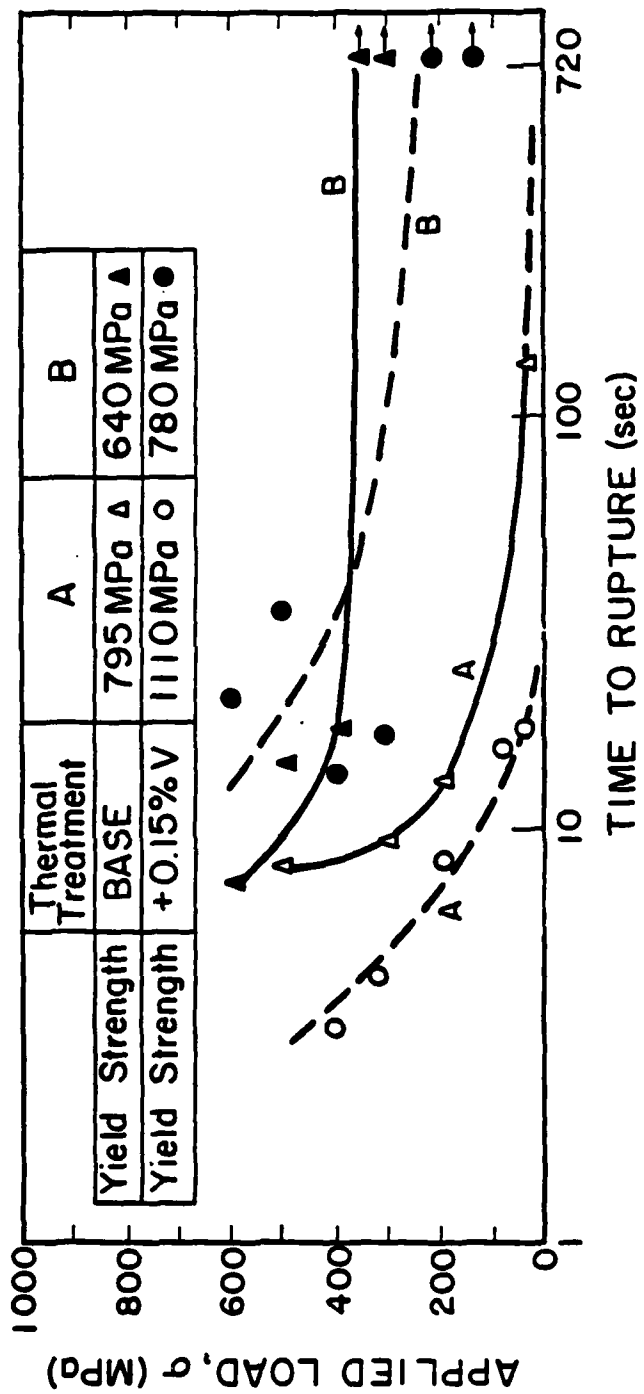


FIG. 20

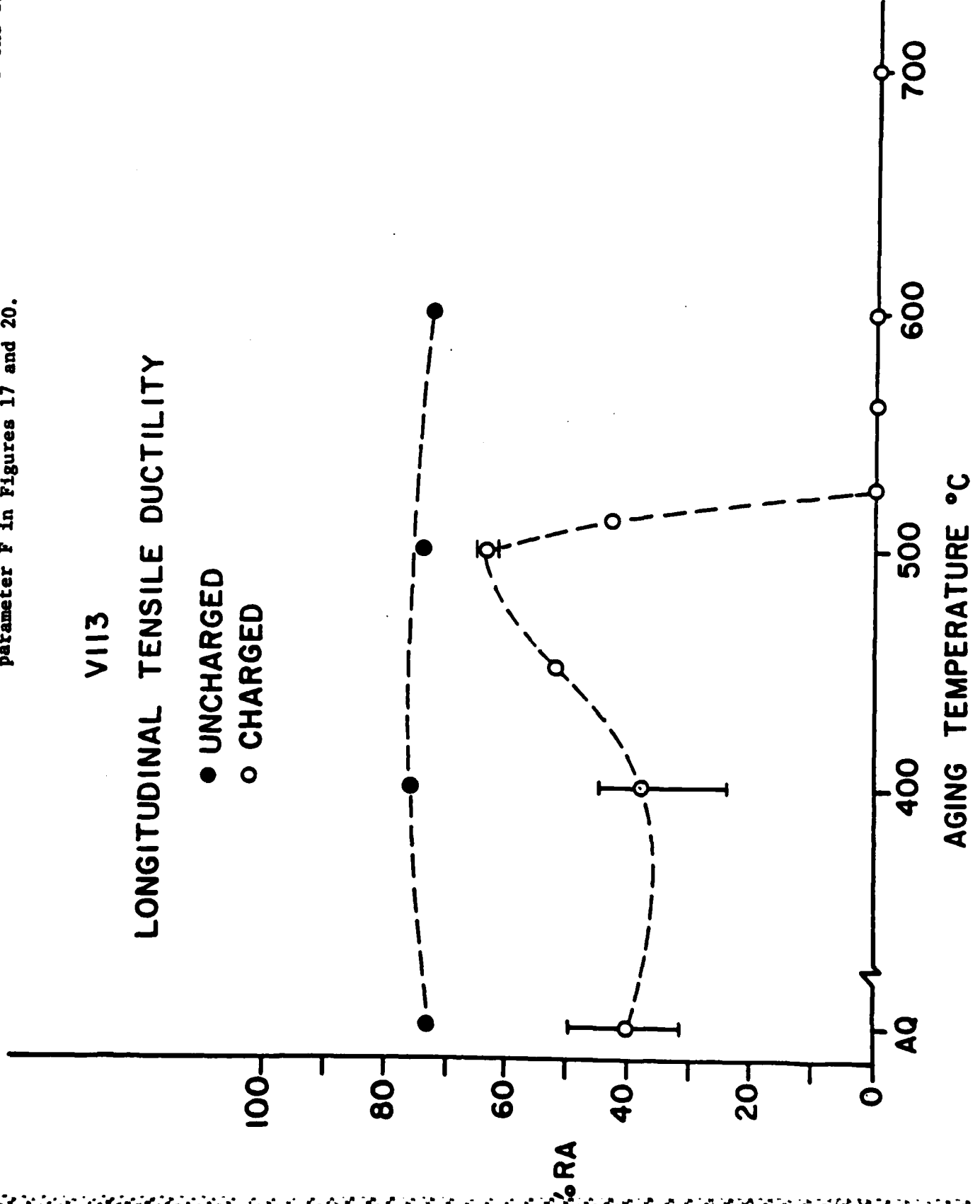
The effect of vanadium bearing traps on the delayed rupture behavior in H_2S NACE solution for two 4140 type steels (as in Fig. 17).

The role of titanium and TiC traps on the hydrogen embrittlement susceptibility of a HSLA type steel. The ordinate is the same as the parameter F in Figures 17 and 20.

VII3

LONGITUDINAL TENSILE DUCTILITY

- UNCHARGED
- CHARGED



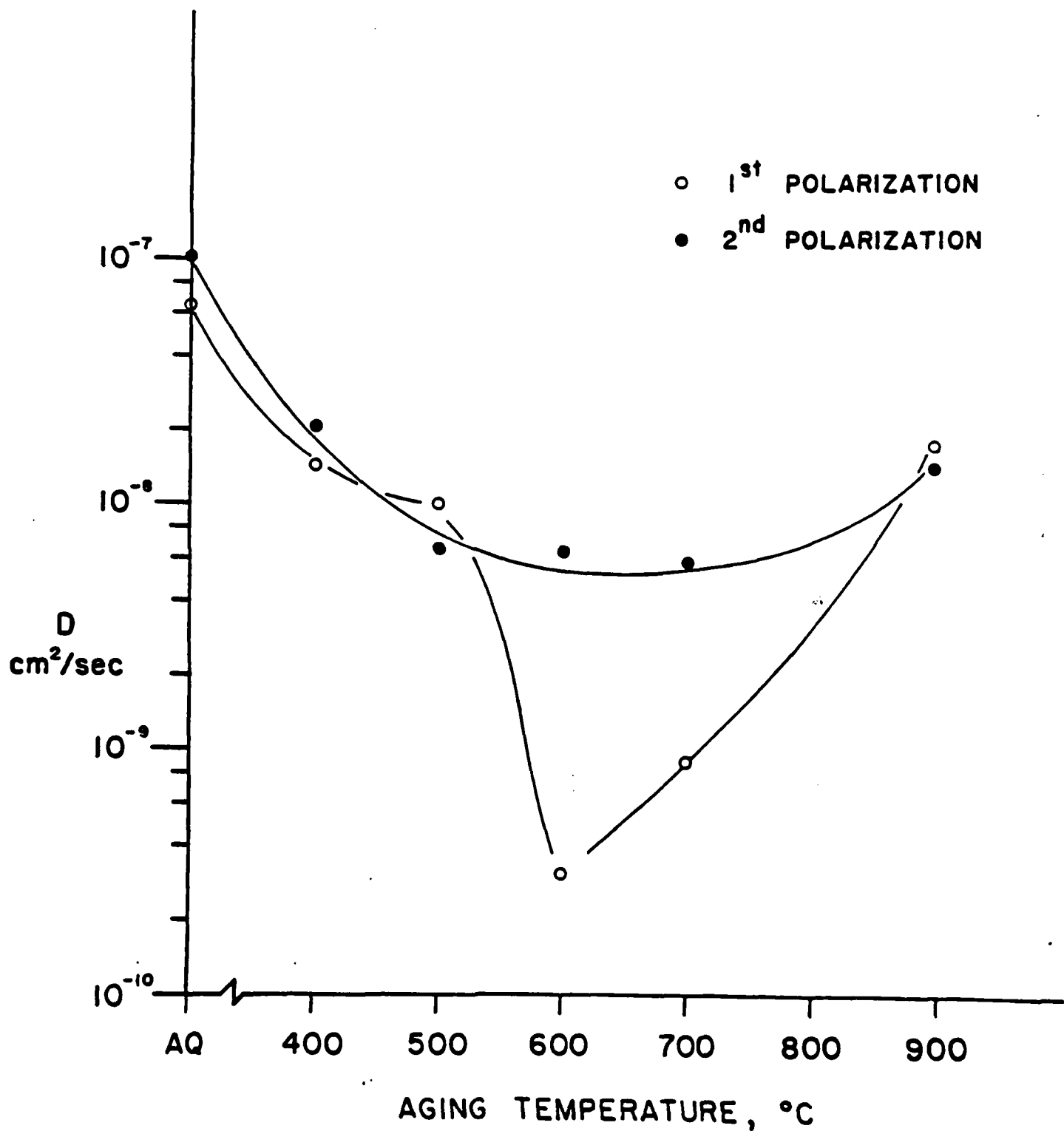
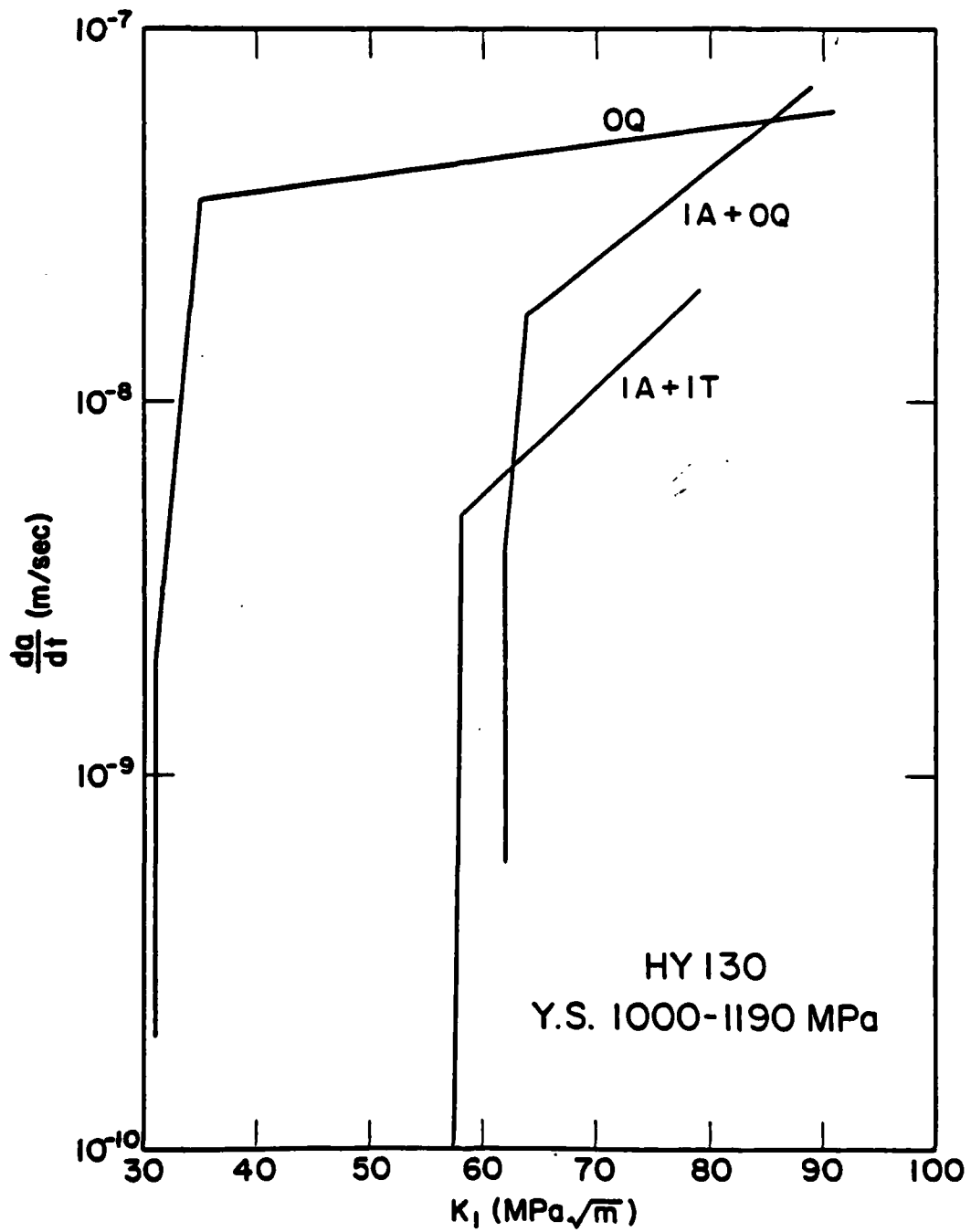


FIG. 22

The effect of trap strength on the effective hydrogen diffusivity.



The effect of heat treatment on stress corrosion crack initiation and growth in 300M and HY130 steels.

FIG. 23 a

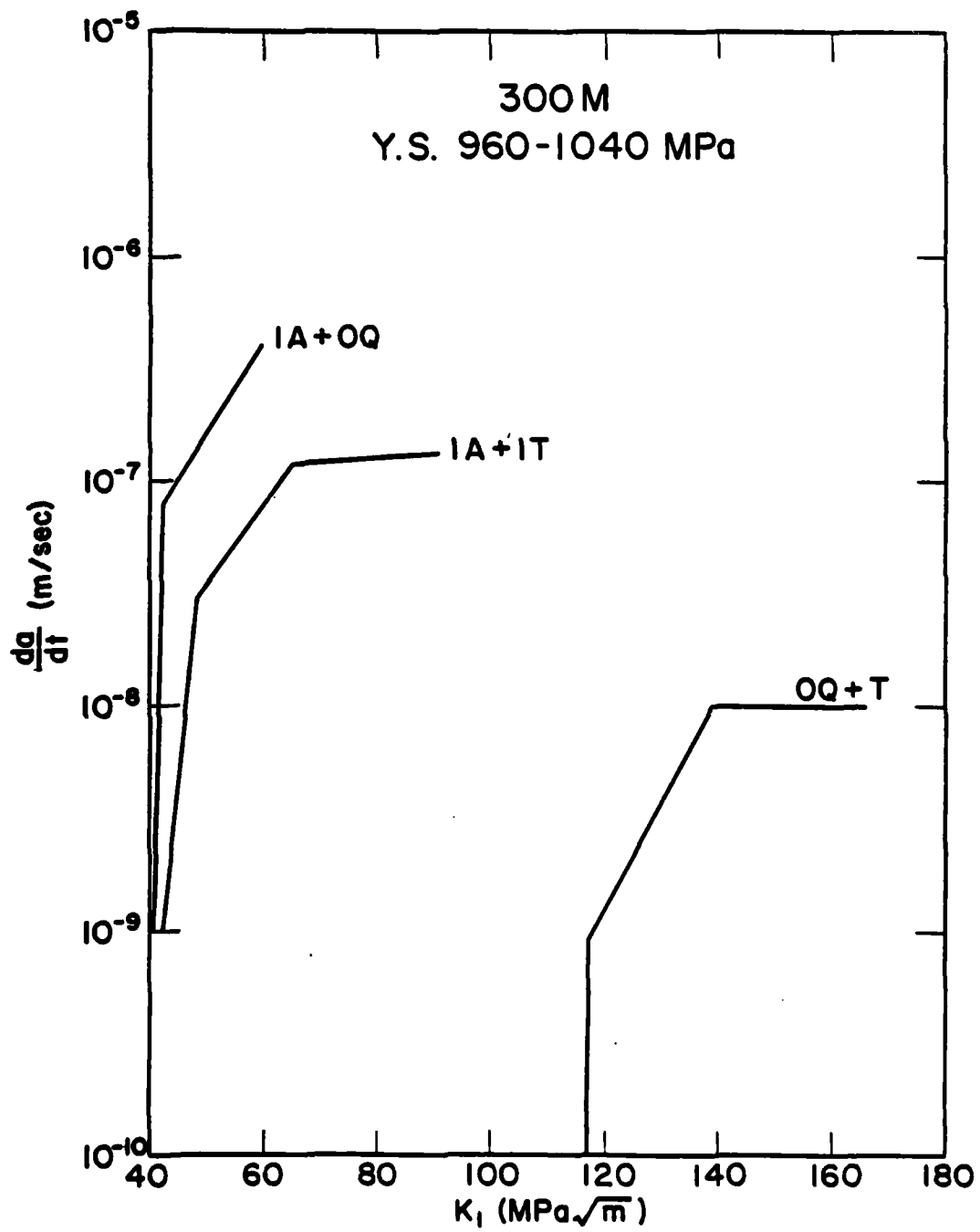


FIG. 23 b

REPORT DOCUMENTATION PAGE		READ INSTRUCTIONS BEFORE COMPLETING FORM
1. REPORT NUMBER NR 036-099-17	N00014-75-C-0265 C-MU	2. GOVT ACCESSION NO. AD-A242 249
4. TITLE (and Subtitle) The Role of Traps in the Microstructural Control of Hydrogen Embrittlement of Steels		3. RECIPIENT'S CATALOG NUMBER
7. AUTHOR(s) I.M. Bernstein and G.M. Pressouyre		5. TYPE OF REPORT & PERIOD COVERED Technical Report
9. PERFORMING ORGANIZATION NAME AND ADDRESS Dept. of Metallurgical Engineering and Materials Science, Carnegie-Mellon University, Pittsburgh, PA 15213		6. PERFORMING ORG. REPORT NUMBER NR 036-099-17
11. CONTROLLING OFFICE NAME AND ADDRESS ONR Code 471 Arlington, VA 22217		8. CONTRACT OR GRANT NUMBER(s) N00014-75-C-0265
14. MONITORING AGENCY NAME & ADDRESS (if different from Controlling Office)		10. PROGRAM ELEMENT, PROJECT, TASK AREA & WORK UNIT NUMBERS
		12. REPORT DATE April 1984
		13. NUMBER OF PAGES
		15. SECURITY CLASS. (of this report) unclassified
		15a. DECLASSIFICATION/DOWNGRADING SCHEDULE
16. DISTRIBUTION STATEMENT (of this Report) Qualified requesters may obtain copies from DDC. Reproduction in part or in whole is permitted for any purpose of the U.S. Government.		
17. DISTRIBUTION STATEMENT (of the abstract entered in Block 20, if different from Report) Unlimited		
18. SUPPLEMENTARY NOTES		
19. KEY WORDS (Continue on reverse side if necessary and identify by block number) microstructure, hydrogen embrittlement, traps, anti-traps, reversible trap, irreversible trap, diffusion, dislocation, interaction coefficient.		
20. ABSTRACT (Continue on reverse side if necessary and identify by block number) Hydrogen can react with heterogeneities in the microstructure of ferrous alloys. These interactions create the necessary sub-steps for failure - crack or void initiation. The nature and type of interactions of hydrogen with the microstructure, combined with the concept of a critical hydrogen concentration for premature embrittlement are discussed. Development of hydrogen resistant steels is possible without compromising critical mechanical properties such as strength ductility, toughness in air and fatigue resistance.		

REPORT DOCUMENTATION PAGE		READ INSTRUCTIONS BEFORE COMPLETING FORM
1. REPORT NUMBER NR 036-099-17	N00014-75-C-0265 C-MU	2. GOVT ACCESSION NO. 3. RECIPIENT'S CATALOG NUMBER
4. TITLE (and Subtitle) The Role of Traps in the Microstructural Control of Hydrogen Embrittlement of Steels		5. TYPE OF REPORT & PERIOD COVERED Technical Report
7. AUTHOR(s) I.M. Bernstein and G.M. Pressouyre		6. PERFORMING ORG. REPORT NUMBER NR 036-099-17
9. PERFORMING ORGANIZATION NAME AND ADDRESS Dept. of Metallurgical Engineering and Materials Science, Carnegie-Mellon University, Pittsburgh, PA 15213		8. CONTRACT OR GRANT NUMBER(s) N00014-75-C-0265
11. CONTROLLING OFFICE NAME AND ADDRESS ONR Code 471 Arlington, VA 22217		10. PROGRAM ELEMENT, PROJECT, TASK AREA & WORK UNIT NUMBERS
14. MONITORING AGENCY NAME & ADDRESS (if different from Controlling Office)		12. REPORT DATE April 1984
		13. NUMBER OF PAGES
		15. SECURITY CLASS. (of this report) unclassified
		15a. DECLASSIFICATION/DOWNGRADING SCHEDULE
16. DISTRIBUTION STATEMENT (of this Report) Qualified requesters may obtain copies from DDC. Reproduction in part or in whole is permitted for any purpose of the U.S. Government.		
17. DISTRIBUTION STATEMENT (of the abstract entered in Block 20, if different from Report) Unlimited		
18. SUPPLEMENTARY NOTES		
19. KEY WORDS (Continue on reverse side if necessary and identify by block number) microstructure, hydrogen embrittlement, traps, anti-traps, reversible trap, irreversible trap, diffusion, dislocation, interaction coefficient.		
20. ABSTRACT (Continue on reverse side if necessary and identify by block number) Hydrogen can react with heterogeneities in the microstructure of ferrous alloys. These interactions create the necessary sub-steps for failure - crack or void initiation. The nature and type of interactions of hydrogen with the microstructure, combined with the concept of a critical hydrogen concentration for premature embrittlement are discussed. Development of hydrogen resistant steels is possible without compromising critical mechanical properties such as strength ductility, toughness in air and fatigue resistance.		

END

FILMED

100-100000-100000

DTIC